UNIVERSITY OF CALIFORNIA SAN DIEGO

Interleukin-17D mediates anti-bacterial immunity in Group A *Streptococcus* infection

A dissertation submitted in partial satisfaction of the requirements for the degree of Doctor of Philosophy

in

Biomedical Sciences

by

Allen Washington, Jr.

Committee in charge:

Professor Jack D. Bui, Chair
Professor John T. Chang
Professor Jeffrey D. Esko
Professor Gerald P. Morris
Professor Christina J. Sigurdson

2019

The dissertation of Allen Washington, Jr. is approved, and it is acceptable in quality and form for publication on microfilm or electronically:

Chair

University of California San Diego

2019

DEDICATION

A mi madre Kyoko

EPIGRAPH

Science is about describing nature, and so is art: We're painting nature.

Polly Matzinger

TABLE OF CONTENTS

LIST OF ABBREVIATIONS

GAS	Group A *Streptococcus*
IL	Interleukin
CCL2	C-C chemokine ligand 2
I.P.	Intraperitoneal
CFU	colony forming units
qPCR	Quantitative real-time polymerase chain reaction
RNA-seq	RNA sequencing
SEM	Standard error of the mean
RAG	Recombinant Activating Gene
TNF	Tumor necrosis factor
INF	Interferon
TLR	Toll-like receptor
PAMP	Pathogen associated molecular pattern

LIST OF FIGURES

LIST OF TABLES

ACKNOWLEDGEMENTS

I would like to acknowledge my mentor Dr. Jack D. Bui for his guidance, patience and support. Jack taught me how to approach challenging projects in biology, develop my original research, and interpret results with caution. Jack's lab environment allowed me to learn from my mistakes, which ultimately had profound impact on my development as a scientist.

I would also like to acknowledge past and present members of the Bui lab: Tim O'Sullivan, Robert Saddawi-Konefka, and Ruth Seelige for generating the foundational data from which my PhD project sprang forth; Semi Han, Yu-jin Jung, Endi Santosa and Calvin Lee for technical support and keeping everything in order; Emilie Gross, Steve Searles, Lindsey Charo, for their helpful discussions, feedbacks, and insightful advices.

I would like to acknowledge my thesis committee: Dr. Gerald Morris, Dr. Christina Sigurdson, Dr. John Chang, and Dr. Jeffrey Esko. These wonderfully patient and generous mentors provided me with counsel and encouragement throughout my PhD.

Finally, I would like to acknowledge my classmates and faculty members I met at UCSD. I am especially grateful to have had the opportunity to perform piano trio pieces in public with School of Pharmacy professors: Dr. Katharina Brandl on the cello, and Dr. Geoffrey Chang on the clarinet. Performing classical music with these gifted faculty members was truly a time well spent outside of lab.

Chapter I is an adapted version of the material published in *Cytokine*. Seelige R, **Washington A Jr**, Bui JD. The ancient cytokine IL-17D is regulated by Nrf2 and mediates tumor and virus surveillance. *Cytokine* 2017; 91:10-12. The dissertation author was the primary author of selected material.

Chapter II is an adapted version of the material that has been prepared for publication. **Washington A Jr**, Shirane K, Chan A, Lee D, Sasaki H, Bui JD. Differential expression analysis downstream of IL-17D. The dissertation author was the primary author of all material.

Chapter III, IV and V are an adapted version of the material that has been prepared for publication. **Washington A Jr**, Varki N, Valderrama JA, Nizet V, Bui JD. IL-17D mediates anti-bacterial immunity in Group A Streptococcus infection. Manuscript in preparation. The dissertation author was the primary author of all material.

Chapter VI is an adapted version of the material that has been prepared for publication. **Washington A Jr**, Seelige R, Wilbur R, Varki N, Bui JD. Spontaneous ulcerative dermatitis in aging IL-17D knockout mice. The dissertation author was the primary author of all material.

VITA

2012	BA, Biology/ BA, Japanese, San Diego State University
2013-2014	The San Diego Foundation Blasker Science & Technology Grant
2014-2016	National Institutes of Health Research Supplement R01CA157885
2016	National Science Foundation East Asia and Pacific Summer Institute
2019	PhD, Biomedical Sciences, University of California San Diego

Publications

Washington A Jr, Varki N, Valderrama JA, Nizet V, Bui JD. IL-17D mediates anti-bacterial immunity in Group A Streptococcus infection. Manuscript in preparation.

Seelige R, **Washington A Jr**, Bui JD. The ancient cytokine IL-17D is regulated by Nrf2 and mediates tumor and virus surveillance. *Cytokine* 2017; 91:10-12.

Saddawi-Konefka R, Seelige R, Gross ET, Levy E, Searles SC, **Washington A Jr**, Santosa EK, Liu B, O'Sullivan TE, Harismendy O, Bui JD. Nrf2 Induces IL-17D to Mediate Tumor and Virus Surveillance. *Cell Report* 2016; 16:2348-58.

Saddawi-Konefka R, O'Sullivan T, Gross ET, **Washington A Jr**, Bui JD. Tumor-expressed IL-17D recruits NK cells to reject tumors. *Oncoimmunology* 2015; 3(12):e954853.

Basa RC, Davies V, Li X, Murali B, Shah J, Yang B, Li S, Khan MW, Tian M, Tejada R, Hassan A, **Washington A Jr**, Mukherjee B, Carethers JM, McGuire KL. Decreased Anti-Tumor Cytotoxic Immunity among Microsatellite-Stable Colon Cancers from African Americans. *PLoS One* 2016; 11(6):e0156660.

ABSTRACT OF THE DISSERTATION

Interleukin-17D mediates anti-bacterial immunity in Group A *Streptococcus* infection

by

Allen Washington, Jr.

Doctor of Philosophy in Biomedical Sciences

University of California San Diego, 2019

Jack D. Bui, Chair

Interleukin-17D (IL-17D) is a cytokine in the IL-17 family that is conserved in vertebrates and invertebrates. In contrast to IL-17A, which is expressed in T cells, IL-17D is expressed broadly in non-immune cells. IL-17D can promote immune responses to cancer and viruses in part by inducing chemokines that recruit natural killer cells and neutrophils. Although bacterial infection can induce IL-17D in fish and invertebrates, the role of mammalian IL-17D in anti-bacterial immunity has not been established. In order to determine whether IL-17D has a role in mediating immunity against bacterial infections, we studied intraperitoneal infection by Group A Streptococcus (GAS) *S. pyogenes* in wild-type (WT) and IL-17D-deficient mice. We found that mice deficient in IL-17D tended to lose more weight and have decreased survival compared to WT animals after GAS infection. In addition, IL-17D deficient animals had increased bacterial burden in the kidney and peritoneal cavity after GAS infection compared to WT animals. In WT animals, IL-17D transcript could be induced by GAS infection, correlating

with increased levels of the chemokine CCL2 and neutrophil recruitment. Notably, GAS-mediated induction of IL-17D required live bacteria, indicating that recognition of physical patterns of the pathogen did not mediate induction of IL-17D. Altogether, our results demonstrate a role for IL-17D in sensing replicating bacteria and inducing immune responses important in clearing bacteria in distant organs.

CHAPTER I: CONSERVATION OF INTERLEUKIN-17 IN ANIMAL IMMUNITY

Conservation of Interleukin-17 in the animal kingdom

Early stage immune responses can dictate the severity and outcome of inflammatory processes such as tumor growth and viral infection. Cytokines such as the interleukin (IL)-17 family cytokines and cellular stress defense (e.g., anti-oxidant) pathways have evolved early and regulate disease surveillance in vertebrates and invertebrates as far back as *Caenorhabditis elegans*. **Fig. 1.1** shows a summary of select animals spanning vertebrates and invertebrates that have been found to express interleukin, IL-17, based on sequence homology.

The role of IL-17 in animal immunity

The IL-17 family of cytokines acts by inducing genes that recruit and activate immune cells (1). Each individual IL-17 cytokine seem to participate in distinct yet overlapping anti-pathogen responses, is induced by different pathways, and can be secreted by immune and non-immune cells. IL-17A and IL-17F are made by Th17 cells and promote inflammatory responses to combat extracellular bacteria and fungi. IL-17C has autocrine activity on epithelial cells to produce antibacterial peptides as well as pro-inflammatory molecules to mediate downstream activities similar to IL-17A/F (1). IL-17E (aka IL-25) is remarkably distinct, attending towards allergic and autoimmune-type (Th2) responses that have risen from the role of anti-parasite immunity. The activities for IL-17B is emerging but seem distinct from other IL-17 family members.

Protein sequence analyses and challenge experiments in teleosts and invertebrates have positioned IL-17 cytokines as early-evolved immune activators, along with tumor necrosis factor (TNF) (2). For example, IL-17 homolog expression, similar to TNF, can be found in invertebrates such as the sea urchin that express few other cytokines and lack chemokines and

interferons (IFNs) (3). Given that invertebrates experience both bacterial and viral infections (4, 5), the lack of IFNs and most other cytokine and chemokine genes suggests that IL-17s (and TNF) must subserve the primordial surveillance of extracellular and intracellular pathogenic insults. Most notably, sea urchin has over 200 TLRs and over 20 IL-17 genes (more than 3 fold compared to human IL-17 genes), which suggests synergistic qualities between the two ancient innate immune activators (3).

In fact, several studies have shown IL-17 homologs to participate prominently in vertebrate and invertebrate innate immunity. Teleosts (e.g., trout) and invertebrates (e.g., oyster) respond strongly to bacterial and viral challenges with a robust increase in IL-17 homologs (2, 4). In particular, IL-17D is highly conserved (>50%) in teleost sequences compared to other IL-17 sequences and constitutively expressed throughout the body in some species such as zebrafish and salmon (2). This observation may indicate a homeostatic role for IL-17D or a distinct function for fish IL-17D; mammalian IL-17D is not constitutively expressed and is not expressed throughout the body in mammals (2).

IL-17D mediates stress response

We have previously demonstrated that IL-17D protects the host by recruiting NK cells to suppress tumor growth (6, reviewed in 7). This is consistent with the observation of elevated IL-17D expression in infected fish and invertebrates, which is essentially a response to an 'abnormal' event that pose danger to the whole organism. We have also previously found that IL-17D is regulated by the transcription factor nuclear factor erythroid-derived 2-like 2 (Nrf2), a well-characterized master regulator that is activated by oxidative and xenobiotic stress (8, 9, reviewed in 10). Nrf2, activated by stress molecules such as reactive oxygen species, acts by turning on anti-oxidant responses. Since IL-17 cytokines developed early in evolution, the

pathway involving IL-17D and Nrf2 suggests an intricate network that involves conserved antioxidant responses and innate anti-pathogen responses. **Fig. 1.2** shows a summary of the regulation and function of the IL-17 family members (adapted from (10)).

IL-17D and Nrf2 confers anti-tumor and anti-viral immunity

In fact, Nrf2 binding site, which are known anti-oxidant response elements (ARE) sequences, are found in the promters and introns of human and murine *il17d* gene (8). Nrf2 binding sites we found corresponded to predicted anti-oxidant response elements (AREs), and accordingly, the oxidative stress inducer hydrogen peroxide and Nrf2 activator *tert*-butylhydroquinone (tBHQ) induced IL-17D in vitro and in vivo. Nrf2 and IL-17D were also upregulated after vaccinia virus (VV) and mouse cytomegalovirus (MCMV) infection of cultured cells and in vivo VV scarification. In cancer cells derived from chemical 3- methylcholanthrene (MCA) tumorigenesis experiments, *il17d*, *Nrf2*, and its known target gene heme oxygenase (*hmox*) 1. Notably, *Il17d*-/- mice were more susceptible to MCA-induced cancer, cleared VV-infected scars slower, and lost more weight after systemic MCMV infection compared to WT animals (8).

Applying a tBHQ-containing skin cream activated Nrf2, and also induced IL- 17D in established tumors. We observed significant inhibition on tumor growth after tBHQ treatment, and this depended on both Nrf2 and IL-17D (8). We could narrow down the effect to be tumor-intrinsic because it was prevented when *nrf2* knock- down or *il17d* deficient cancer cells were transplanted. We had previously shown that forced expression of IL-17D in tumor cells induced rejection by recruiting tumor-fighting NK cells (6, 7). Similarly, topical application of tBHQ cream recruited NK cells to tumors, and this was prevented if the tumors lacked Nrf2 or IL- 17D (8).

We had hypothesized that the presence of IL-17D orthologs in invertebrate species that lack most other cytokines, including IFNs, meant that IL-17D must have anti-pathogen activity. Our previous studies confirm that IL-17D is required for optimal antiviral immunity (8, 9). Whether it also participates in immunity against other pathogens, such as intracellular bacteria, is not known. Although we have identified NK cells as a primary target for IL-17D, it is likely that other antiviral pathways are induced by IL-17D. Further studies on the genes induced downstream of IL-17D will elucidate the mechanism of how it protects the host from viral infection. We speculate that similar to IL-17C's induction of defensins and anti-bacterial cathelicidins, IL-17D should induce antiviral genes such as nucleases or other IFN-induced genes. Moreover, as we have found that tBHQ can induce Nrf2 and IL-17D in the therapy of cancer, this strategy could work for local viral infection.

Outside of infection, Nrf2 and IL-17D also influence cancer progression. Notably, Nrf2 has been puzzling researchers for decades as a 'double-edged' sword that can either promote or inhibit cancer (23, 73). It is proposed that Nrf2 can either be anti-tumorigenic, by mediating protection of normal cells against carcinogens, or pro- tumorigenic, by protecting cancer cells from oxidative stress. Our finding that Nrf2 also induces IL-17D adds a further layer of complexity to its pro- and anti-tumor activities. Importantly, our studies have confirmed that inducing Nrf2 and IL-17D in established cancers can lead to recruitment of NK cells and cancer regression. Therefore, we conclude that the anti-tumor activities of Nrf2, when bolstered through induction of IL-17D, can outweigh its pro-tumor activities in our mouse model. As we elucidate other regulators of IL-17D and its effector pathways, we can tailor specific therapies to activate only the anti-tumor activities of Nrf2 and/or IL-17D.

In summary, by showing that Nrf2 and IL-17D are induced after viral infection and that IL-17D is required for optimal anti-viral responses, we propose that the Nrf2/IL-17D axis evolved as a mediator of immunity, specifically against intracellular pathogens. Inducing IL-17D via the activation of Nrf2 by tBHQ might be broadly applicable for the treatment of viral infection and serve as an immune therapy similar to the observed application in murine cancer. The specific involvement of Nrf2 and IL-17D in other types of infection as well as other types of (human) cancers still needs to be determined and will remain an active area of investigation in the future.

Chapter I, in part, is an adapted version of the material published in: Seelige R, **Washington A Jr**, Bui JD. The ancient cytokine IL-17D is regulated by Nrf2 and mediates tumor and virus surveillance. *Cytokine.* 2017;91:10-12. The dissertation author was a co-first author of the manuscript.

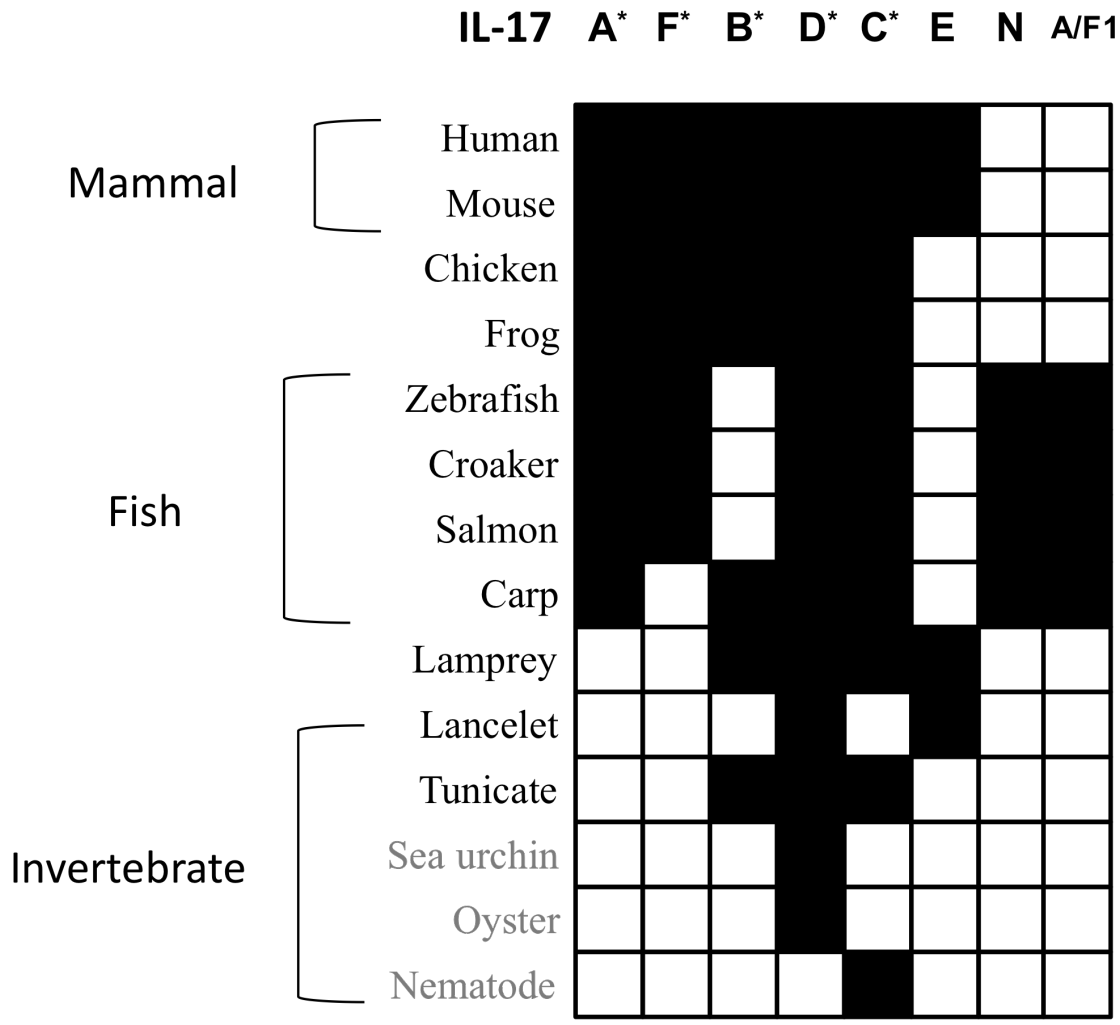

Figure 1.1 IL-17 in the evolution of animal immunity. The presence (black) or absence (white) indicates presence of each IL-17 homolog (IL-17A, IL-17F, IL-17B, IL-17D, IL-17C, and IL-17E (aka IL25)) cytokines in vertebrates and invertebrates. IL-17N and IL17A/F1 are exclusively found in teleosts. Identification of additional IL-17 homologs in sea urchin, oyster, and nematode are still ongoing.

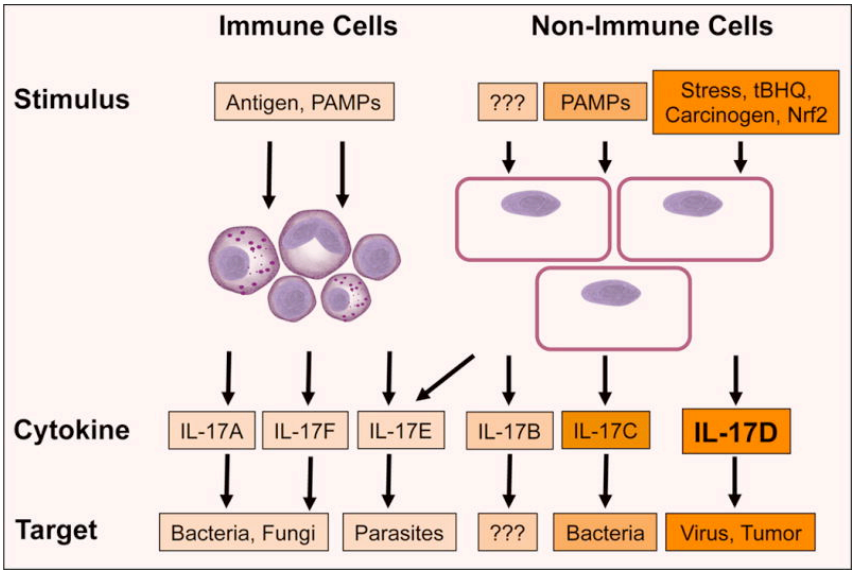

Figure 1.2 IL-17 in the evolution of animal immunity. Previous work by colleagues in the Bui lab uncovered a novel role for IL-17D in surveillance of nascent tumors and viral infection. Oxidative stress by tBHQ (tert-butyl hydroquinone) activates the anti-oxidant transcription factor, Nrf2, which induces IL-17D expression. IL-17 cytokines are known to mediate anti-pathogen responses by active secretion from immune cells and/or non-immune cells.

CHAPTER II: INTERLEUKIN-17D-INDUCIBLE GENES

2.1 Introduction

The circumstance for a cancer cell to grow, metastasize, or reject is contingent on its interactions with the non-neoplastic tumor microenvironment and the immune system. The complex interactions between immunity and cancer involve signal molecules such as chemokines and cytokines that modulate wound healing, immune cell infiltration, and/or neoplastic cell growth. Previously published data by O'Sullivan and colleagues studied in detail the transcriptomic divergence between highly immunogenic rejection-inducing sarcomas (regressors) and the weakly immunogenic sarcoma cells (progressors) (11). Regressors ('unedited') tumors are derived from *Rag-/-* immune deficient mice, while progressors ('edited') can be derived from WT or immune deficient mice (12). Of particular interest, a pro-inflammatory cytokine IL-17 family member, IL-17D, was highly expressed in certain regressors and poorly expressed in progressors (6). Furthermore, IL-17D was demonstrated to promote regression or growth delay of progressors when forcedly expressed in sarcomas and melanomas (6, reviewed in 7).

IL-17 cytokines have been mostly found to exhibit pro-inflammatory roles (13,14). IL-17A and IL-17F bind the same IL-17RA/RC receptor complex; IL-17C activates downstream signaling through the IL-17RA/RE complex; IL-17E and IL-17B both bind IL-17RB. All three receptor complexes described above (RA/RC, RA/RE, RA/RB) are known to activate the signaling molecule NF-κB through Act1-TRAF6-TAK signaling, and thus share common effector functions such as inducing similar sets of chemokines (15).

Although the receptor complex for IL-17D is not known, Starnes and colleagues have

found that this cytokine functionally overlaps with IL-17A in that it induces NF-κB-associated canonical effectors such as IL-6 and GM-CSF in human endothelial cells (16). Additionally, O'Sullivan and colleagues have found CCL2, a chemokine also downstream of IL-17A, to be induced by IL-17D in mouse endothelial cells (6). We also over-expressed IL-17D in melanoma cells and detected higher CXCL10 (**Fig. 2.2A**), a chemokine known to recruit T cells and is inducible by cytokines such as IFN-γ and IL-17A (17,18). Since genes such as *Il6*, *Ccl2*, and *Cxcl10* have more than one inducer, whether there are uniquely IL-17D-dependent genes are currently not known. In order to determine whether there are non-overlapping IL-17D-induced versus IL-17A-induced genes, we performed a differential expression analyses on extracted mRNA from IL-17A- versus IL-17D- stimulated cell lines. In these experiments, we utilized mouse endothelial (SVEC) and mouse melanoma (B16) cell lines, since we previously demonstrated these cell types to respond to IL-17D (6) (**Fig. 2.2B**).

Results

2.2.1 IL-17D induces canonical pro-inflammatory molecules

In order to establish whether recombinant IL-17D used in our RNA-seq experiment was functional, various non-immune cells (e.g., fibroblasts, myocytes) in addition to bone marrow-derived macrophage (BMDM) were stimulated in vitro with IL-17D. First we confirmed that IL-17D induces Ccl2 in fibroblasts, similar to the degree by IL-17A and IL-17C (**Fig. 2.1A**). Although IL-17D did not induce Ccl2 in macrophage (not shown), canonical inflammatory activity was detected by measuring the transcript level of IL-6 (**Fig. 2.1B**). IL-17D protein from mouse sequence shares high homology to rat sequence (78% identical), and thus mouse IL-17D was sufficient to induce *Il6* in rat myocytes (**Fig. 2.1C**). These data demonstrated the functionality of the recombinant IL-17D used in our RNA-seq experiment.

In order to select the cell line to be used in RNA-seq, we considered B16 due to detecting autocrine/paracrine response to over-expressed IL-17D from transduced cell line. We performed microarray analysis by detecting differential gene expression in IL-17D-expressing B16 cells versus control cells. First, over-expressed IL-17D transcript was confirmed to be higher in B16.17D cells compared to parent B16.ctrl (~4 fold) in the microarray data (**Fig. 2.2A**). We found one chemokine (CXCL10) positively correlated with the expression of IL-17D in B16 cells (**Fig. 2.2A**). In our following qPCR experiment, GFP overexpressing cell line (B16.gfp) was used as a control to confirm the microarray result, comparing against B16.17D. *Cxcl10* transcript was consistently higher (>6 fold) in B16.17D compared to control in qPCR experiments, which confirmed the result of the microarray study (**Fig. 2.2B**). There was no difference in *Ccl2* transcript between B16.17D and control B16 cells in both microarray and qPCR experiments (not shown).

2.2.2 IL-17D and IL-17A induces some overlapping genes

To investigate the downstream genes of IL-17D by RNA-seq, we stimulated endothelial cells (SVEC) and melanoma cells (B16) with either recombinant IL-17D or IL-17A. We observed that IL-17D and IL-17A largely has an inducing effect on SVEC, with minimal down-regulated genes (**Fig. 2.3A**). IL-17A is known to induce a suite of chemokines, including *Ccl2*. As expected, our RNA-seq data confirmed both IL-17A and IL-17D to have the effect of inducing *Ccl2* in endothelial cells (**Supplemental Table I**). Unexpectedly, we detected more down-regulated mRNA than induced genes in B16 cells (**Fig. 2.3B, Supplemental Table II**). However, consistent with our microarray result, our RNA-seq data also found that IL-17D (and IL-17A) induced *Cxcl10* in B16 cells (**Supplemental Table II**). Overall, we found that 11 genes: *Ccl2*, *Cxcl1*, *Hmga1*, *Zc3h12a*, *Cebpd*, *Nfkbiz*, *Ier3*, *Erdr1*, *Itpk1*, *Chst7*, and *H2afj* were

commonly induced by IL-17A and IL-17D in SVEC cells (**Supplemental Table I**). In contrast, only 3 genes: *Cxcl10*, *L1cam*, and *Slc7a11* overlapped between IL-17A- and IL-17D-stimulated B16 cells (**Supplemental Table III)**.

2.2.3 IL-17D induces melanosome-associated genes

Next we re-analyzed the data by sorting differentially expressed genes that are exclusive to IL-17D. We found genes such as *Pax3* and *Dct* were specifically induced only by IL-17D in SVECs (**Fig. 2.4A**). We further re-analyzed the data set by combining SVEC and B16 into one output, and found 178 genes to be induced by IL-17D (**Fig. 2.4B**). Separately, we found that in The Cancer Genome Atlas (TCGA), 780 genes are positively-correlated with IL-17D expression in melanoma. Between our RNA-seq data and available TCGA data set, 8 genes were found to be consistently positively correlated with IL-17D expression, including *Dct*, *Pax3*, and *Sox10* genes. We sought to confirm our result by stimulating various cell lines with IL-17D. We found IL-17D to induce *Dct* and *Sox10* in SVEC (**Fig. 2.5A, 2.5B**). *Pax3* was confirmed to be induced by IL-17D in MEF (**Fig. 2.5C**).

2.3 Discussion

Differentially regulated genes by IL-17D in endothelial cells versus melanoma cells were identified and confirmed in our analyses through microarray and RNA-seq. As expected, differences in response to IL-17D versus IL-17A were less distinct for chemokines such as *Ccl2* and *Cxcl10*, which are part of canonical pro-inflammatory responses. Both IL-17D and IL-17A induced *Ccl2* in endothelial cells; *Cxcl10* in melanoma. In contrast, IL-17D but not IL-17A induced dopachrome tautomerase (Dct). We were able to confirm through qPCR that *Dct* is indeed induced in endothelial cells, although not in macrophages, which suggests a tissue-specific function of non-immune cells that is dependent on cytokines such as IL-17D. *Dct* is part

of the melanosome, which is responsible for melanin production in melanocytes and is typically involved in the physiological regulation of pigmentation, along with other genes such as tyrosinase. In fact, in our RNA-seq data, we found SVEC stimulated by IL-17D had a higher transcript level of genes involved in melanogenesis, such as *Dct*, *Gpnmb*, *Mlana*, *Mlph*, *Pmel*, and *Pax3* (**Fig. 2.3**).

Melanocytes receive secreted factors (e.g., cytokines and growth factors) from cells such as endothelial cells, fibroblasts, and keratinocytes, in addition to hormonal signals, to initiate melanin synthesis (19). Melanogenesis is regulated by transcription factors such as *Pax3* and *Sox10* (20), which we also found to be downstream of IL-17D.

Melanin production holds importance not only in the context of a photoprotective and antioxidant role in the skin, but also as a modulator of inflammation (21). Our observation of IL-17D inducing the 'melanosome' genes may be related to our previous findings on Nrf2 inducing IL-17D (summarized in Chapter I). Nrf2 is a transcription factor essential in anti-inflammatory efforts and antioxidant effects (22, 23). We speculate that therefore antioxidant response, melanin synthesis, and immune cell recruitment (e.g., by IL-17D) are intertwined vestigial cellular protective mechanism present in animal species. Our data here in Chapter II suggests that IL-17D may be one of many cytokines that are secreted by the melanocyte environment (e.g., keratinocytes) to promote protective melanin synthesis.

Chapter II is an adapted version of the material that has been prepared for publication. **Washington A Jr**, Shirane K, Chan A, Lee D, Sasaki H, Bui JD. Differential expression analysis downstream of IL-17D. The dissertation author was the primary author of all material.

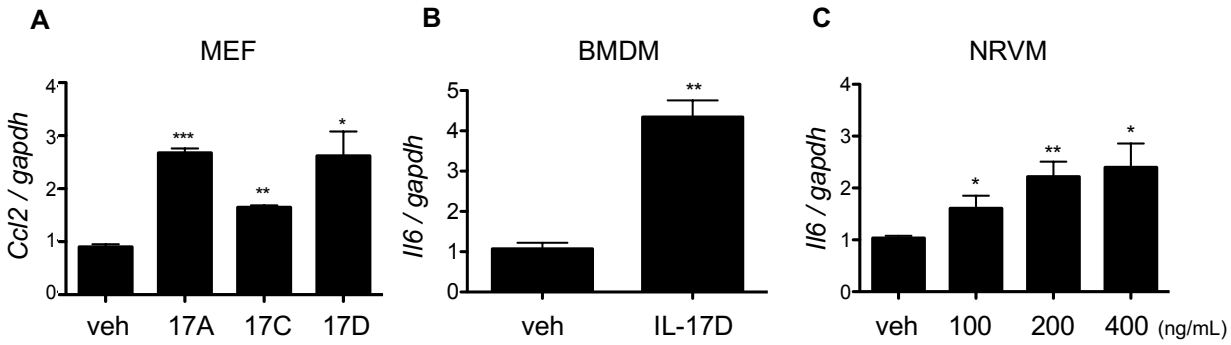

Figure 2.1 recombinant IL-17D stimulates cells to express canonical pro-inflammatory effectors. (**A**) Ccl2 transcript measured in mouse embryonic fibroblast stimulated with 100ng/mL IL-17A, IL-17C or IL-17D for 3 hours. (**B**) Il6 transcript measured in bone marrow-derived macrophage from wild-type C57BL/6 mice stimulated with 50ng/mL IL-17D for 2 hours. (**C**) Il6 transcript measured in neonatal rat ventricular myocytes stimulated with 100-400 ng/mL IL-17D for 3 hours. Data shown are mean and SEM. *, $P < 0.05$; **, $P < 0.01$; ***, $P < 0.001$.

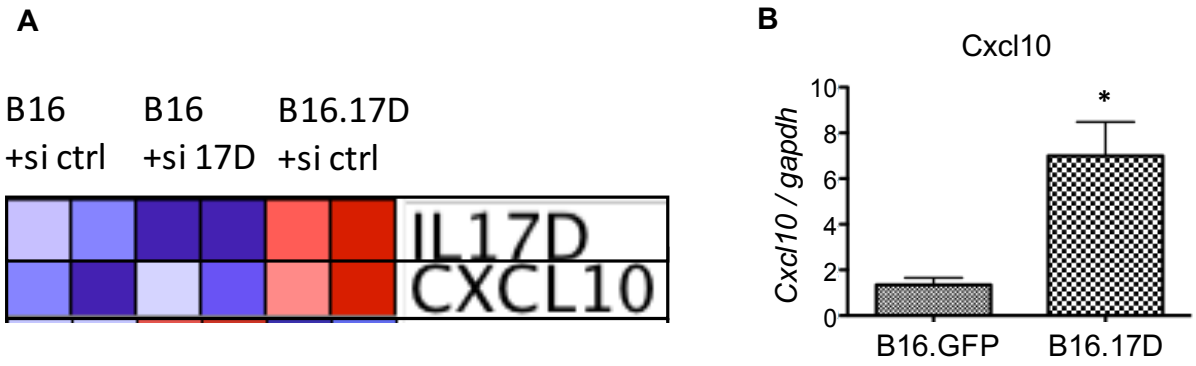

Figure 2.2 Canonical pro-inflammatory genes are highly expressed in IL-17D overexpressing cell line. (**A**) Microarray of B16 cell line parent control versus transduced IL-17D over-expressor. siRNA directed at random sequence or Il17d was introduced to B16 parent; Over-expressor cell line (B16.17D) received the siRNA control only. (**B**) Cxcl10 transcript measured by qPCR in B16 cell line comparing GFP versus IL-17D over-expressor. Data shown are mean and SEM. *, $P < 0.05$

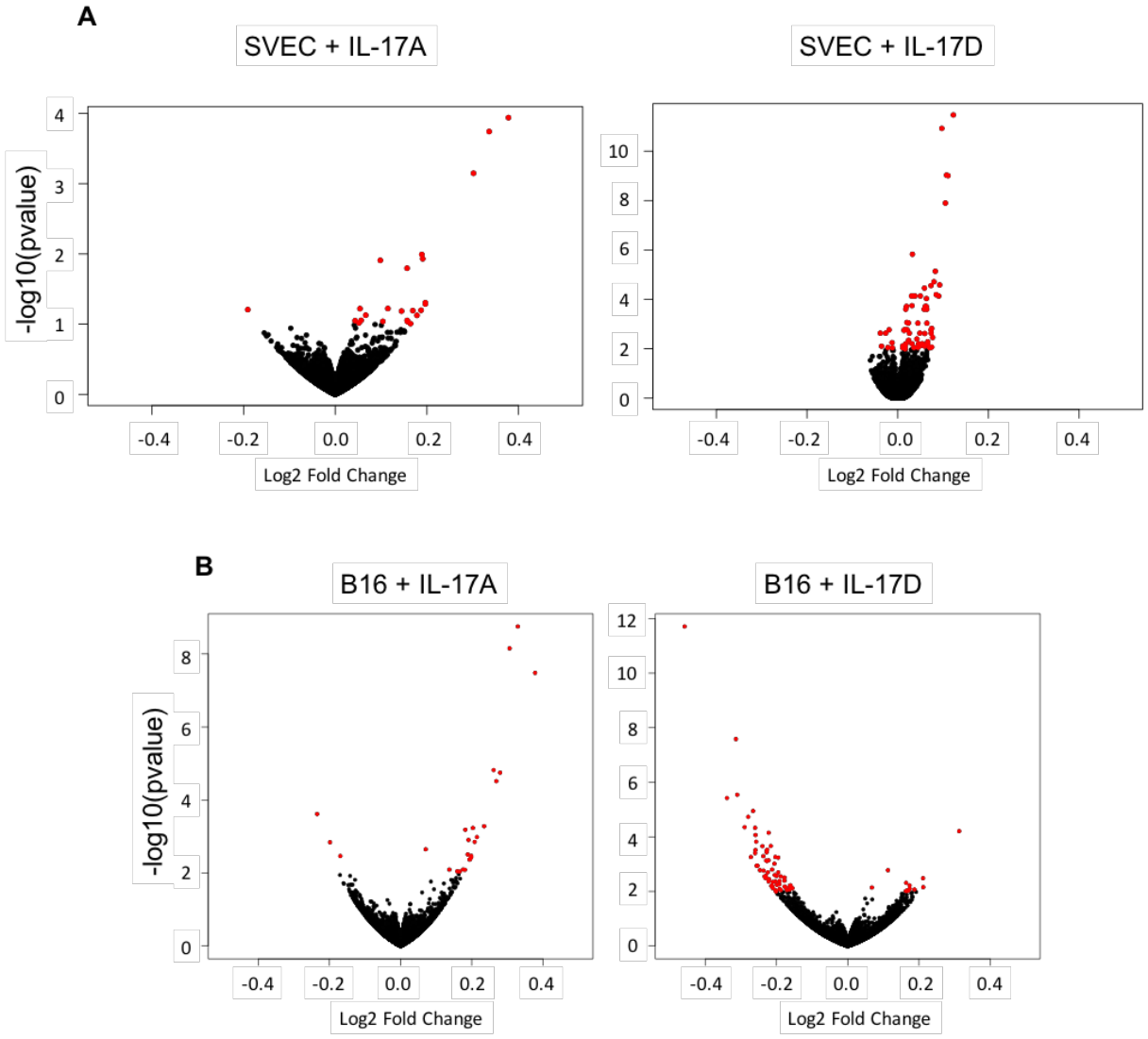

Figure 2.3 Genes are differentially induced or suppressed in cells stimulated with IL-17D versus IL-17A. RNA-seq volcano plot of genes differentially regulated ($p<0.01$ marked red) by IL-17D and IL-17A in (**A**) SVEC and (**B**) B16 cell lines compared to vehicle treatment.

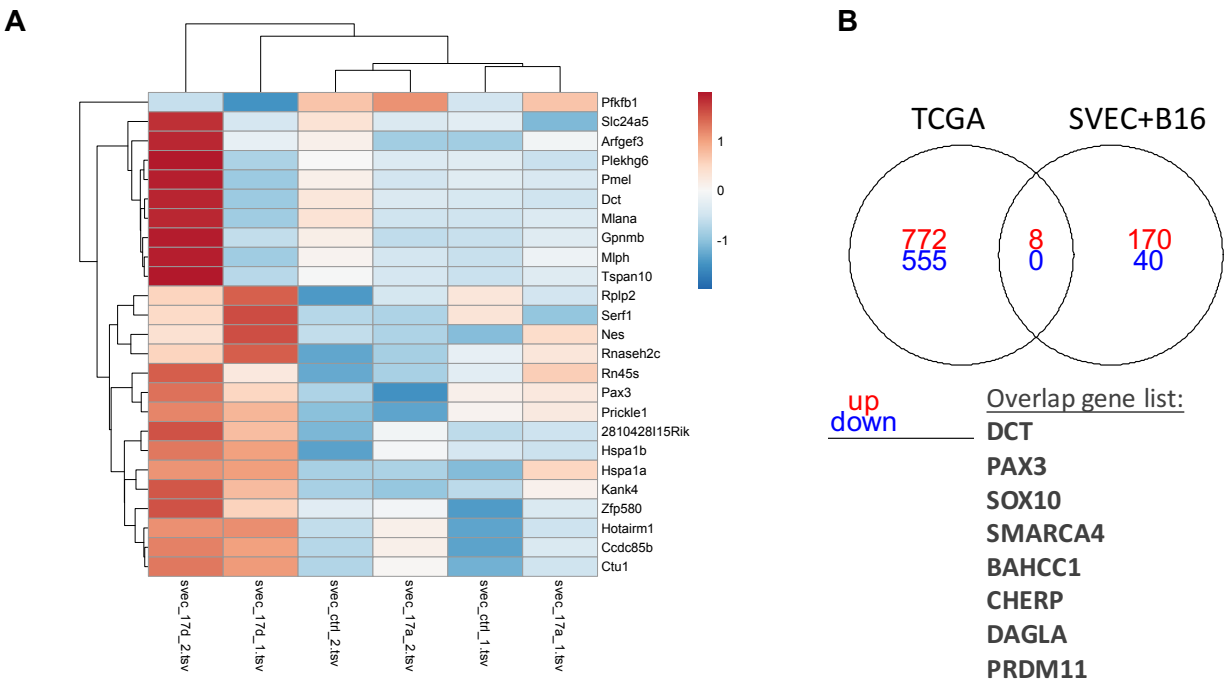

Figure 2.4 RNA-seq discovers non-canonical IL-17D-dependent genes in non-immune cells. (**A**) Differntially expressed genes (adjusted $p < 0.001$) in endothelial cells stimulated by IL-17D for 6 hours (each lane is pooled triplicate) over vehicle and IL17A-treated cells. (**B**) Overlap between genes that are linked with IL-17D expression in The Cancer Genome Atlas (TCGA) and genes positively-regulated by IL-17D in combined datasets from B16 and SVEC.

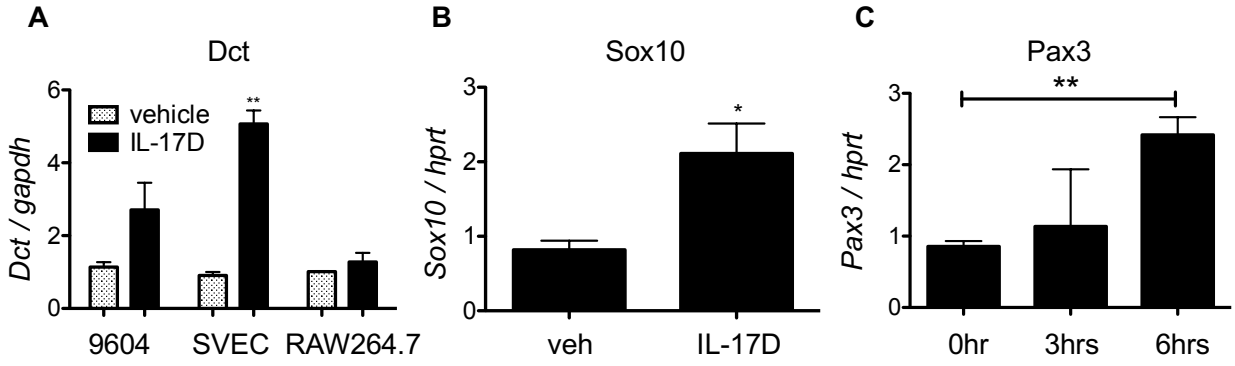

Figure 2.5 IL-17D induces melanogenesis-associated genes in non-immune cells. (**A**) Dct transcript measured in sarcoma cell (9604), endothelial cell (SVEC), and macrophage (RAW264.7) after 3 hours of IL-17D incubation in medium versus vehicle treatment. (**B**) Sox10 transcript measured in SVEC after incubation with IL-17D for 6 hours. (**C**) Pax3 transcript measured in mouse embryonic fibroblast (MEF) stimulated with 100ng/mL IL-17D. Data shown are mean ± SEM. *, $P < 0.05$; **, $P < 0.01$

CHAPTER III: INTERLEUKIN-17D PROMOTES SURVEILLANCE OF GROUP A STREPTOCOCCUS INFECTION

3.1 Introduction

Interleukin (IL)-17 cytokines include 6 members (A-F) that exhibit functional roles in inflammation, autoimmunity, and cancer (14, 15). In contrast to IL-17A and IL-17F that are mostly expressed in T cells, IL-17D is expressed broadly in non-immune cells (16). IL-17B and IL-17C are also expressed in non-immune cells and furthermore, are known to induce similar sets of genes that are downstream of IL-17A (16, 24-26). IL-17A and IL-17C have been shown to protect the host from various bacterial species in experimental infection models (26-31). On the other hand, IL-17E (aka IL-25) promotes immune responses against parasites (32). Although IL-17B antagonizes IL-17E-mediated inflammation, it is less defined individually in its role in anti-pathogen response (33).

The role of IL-17D in anti-bacterial immunity is relatively unexplored in mammals. However, various research involving fish and invertebrate animal models have uncovered a positive role for IL-17D homologs in anti-bacterial immune responses (2-5, 34-38). Although most species of fish exhibit constitutive IL-17D expression in various organs, *Il17d* expression increases in response to bacteria in organs such as the skin and head kidney (3, 34). In addition to live bacteria, bacterial components such as LPS can induce in vitro *Il17d* in skin cells of lampreys in vitro (35). Bacteria seems to induce *Il17d* expression in invertebrates such as mollusks and amphioxus as well (4, 36-38). Therefore, we asked whether IL-17D has a role in mediating immunity against bacterial infections in mammals. We employed an intraperitoneal infection model to study anti-bacterial responses against Group A Streptococcus (GAS). In order to study the endogenous activity of IL-17D in anti-microbial immunity, we first sought to

determine survival and weight loss in IL-17D-deficient mice compared to wild-type mice. Previously, Seelige and colleagues demonstrated higher viral burden in organs of *Il17d*-/- mice compared to WT mice (9). Thus, some organs that are IL-17D deficient may succumb to worse infection by pathogens than WT. We therefore investigated bacterial burden in organ homogenates of GAS-infected mice as a result of lacking IL-17D expression.

3.2 Results

3.2.1 Anti-bacterial immunity is compromised in Il17d-/- mice

In order to determine whether IL-17D has a role in mediating immunity against bacterial infection, survival and weight loss was monitored in mice infected by group A Streptococcus. Absence of *Il17d* transcript was confirmed in the knockout organ by qPCR (**Fig. 3.1A**). We observed trends in decreased survival in mice lacking IL-17D (**Fig. 3.1B**). The weight loss in the knockout mice followed the modest trend of survival. Although no difference in weight loss was detected after inoculating mice with $5x10^6$ GAS (**Fig. 3.2A**), relatively higher dose of $10x10^6$ and $20x10^6$ GAS elicited noticeable, yet non-significant, differences in weight loss (**Fig. 3.2B, 3.2C**). Previously we had observed that *Il17d*-/- mice manifest higher viral burden in some organs after MCMV infection (9). We hypothesized that some organs would contain a higher bacterial burden when IL-17D is absent. We determined the optimal assay time point to be at 24 hours, since we did not detect difference at earlier (5hr) time points, but detected significant difference at 24 hours (**Fig. 3.3A, 3.3B**). We found that some organs such as the kidney and peritoneal cavity harbored significantly higher GAS colony forming units (CFU) in the *Il17d*-/- mice (**Fig. 3.3B, 3.4B**). At 24 hours, we detected significantly higher bacterial burden in the kidneys of *Il17d*-/- mice compared to WT mice using three different GAS doses, $6x10^6$, $8x10^6$, and $10x10^6$ (**Fig. 3.3C, 3.3D**). Although we saw higher burden in *Il17d*-/- kidney and

peritoneum, other organs such as lung and heart did not exhibit difference in GAS burden (**Fig. 3.4A-H**). We also did not measure significant differences between *Il17d*-/- and WT in bacterial burden post 76- and 96- hours i.p. GAS infection in organs examined (**Fig. 3.5A, 3.5B**).

3.3 Discussion

We demonstrated in Chapter II that IL-17D shares similar downstream pro-inflammatory effectors (such as Ccl2, Cxcl10) with cytokines such as IL-17A and IL-17C. The slight decrease in *Il17d*-/- survival after GAS infection suggested that IL-17D may have overlapping functions with other cytokines that compensated for the absence of IL-17D. The overt phenotype is therefore likely spared in the absence of IL-17D in GAS-infected mice. However, we saw higher GAS burden in the *Il17d*-/- kidney, which suggests an organ-specific program that may depend more heavily on IL-17D for anti-bacterial immunity.

The phenotype of lacking IL-17D was limited to some organs such as the kidney and peritoneum, as we did not see major differences in bacterial burden in organs such as the spleen and lung. Our data suggests IL-17D is expressed in the kidney and has a protective effect in bacterial infection, especially within 24 hours. Although IL-17C is also expressed in kidney epithelial cells, it has been reported to exacerbate inflammation (39). Experimental fungal infection found *Il17c*-/- mice to have higher survival compared to WT, suggesting a role for IL-17C in exacerbating tissue damage and inflammation (39). Although IL-17 receptors, IL-17RA and IL-17RC, are protective in candidiasis, IL-17RE (which binds IL-17C) does not confer protection (40), which further strengthens the view that IL-17C does not play a role in the resolution of the disease, unlike IL-17A/F. However, protective inflammation may transgress into excessive inflammation especially during the resolution and recovery phase of tissue injury. For example, although IL-17A promotes neutrophil migration and is known generally to have

anti-pathogen immunity, lacking IL-17A is protective in an ischemia-reperfusion injury model (41). Functionally, IL-17s overlap; however, the degree of inflammation promoted by each seem to be at a different scale. Both IL-17C and IL-17A/F, for example, promotes LPS-induced toxic shock, while IL-17D does not (42-44). In light of these previous findings, we speculate that the modest effect of IL-17D is attributable in part to the complex overlaps in function to other pro-inflammatory cytokines that leads to similar downstream effectors to control the degree of inflammation. As we did not observe significant increases in death and weight loss in *Il17d*-/- mice upon opportunistic GAS infection, we speculate that compensatory mechanisms for immune cell recruitment exists due to functional overlap between other pro-inflammatory cytokines and IL-17D.

Chapter III, in full, is an adapted version of the material that has been prepared for publication. **Washington A Jr**, Varki N, Valderrama JA, Nizet V, Bui JD. IL-17D mediates anti-bacterial immunity in Group A Streptococcus infection. Manuscript in preparation. The dissertation author was the primary author of all material.

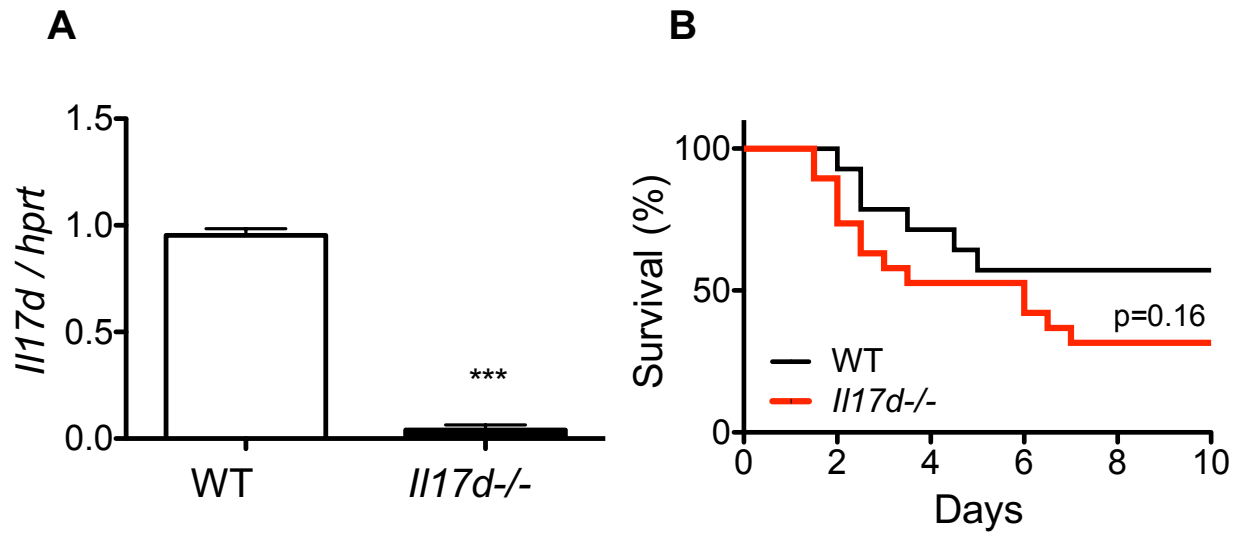

Figure 3.1 IL-17D knock-outs trend in higher deaths compared to wild-type animal. (**A**) Il17d transcript measured in peritoneal tissue (n=3) from wild-type C57BL/6 (WT) and Il17d-/- mice. (**B**) Percentage survival of Group A Streptococcus-infected (i.p. $5x10^7$) WT and *Il17d-/-* mice were monitored for survival (WT, n=14; *Il17d-/-*, n=19). Data shown are mean ± SEM. ***, $P < 0.001$.

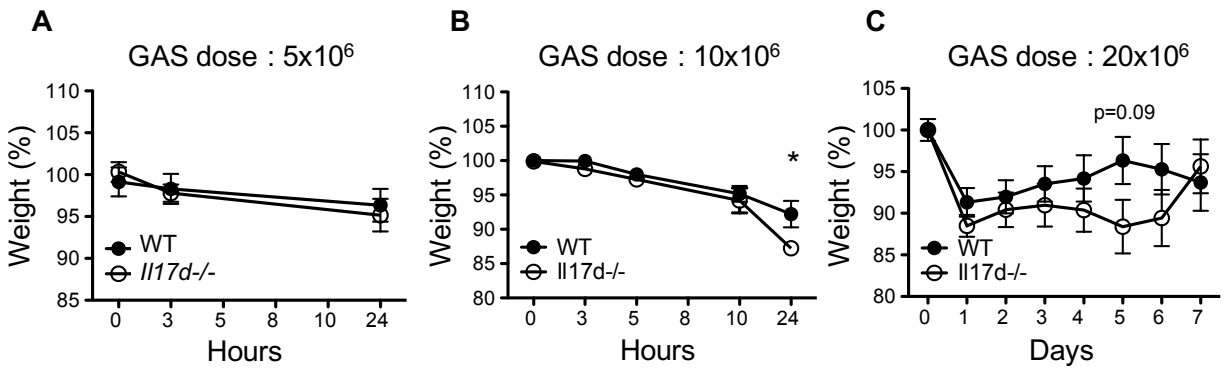

Figure 3.2 IL-17D knock-outs trends in higher loss of weight compared to wild-type animal. (**A**) Weights of 8-12week old WT and *Il17d-/-* mice after 24 hours post- i.p. $5x10^6$ GAS or (**B**) 24 hours post- i.p. $10x10^6$ GAS or (**C**) 7 days post i.p. $20x10^6$ GAS. Data shown are mean ± SEM and are combined data of at least n=6 per group. *, $P < 0.05$.

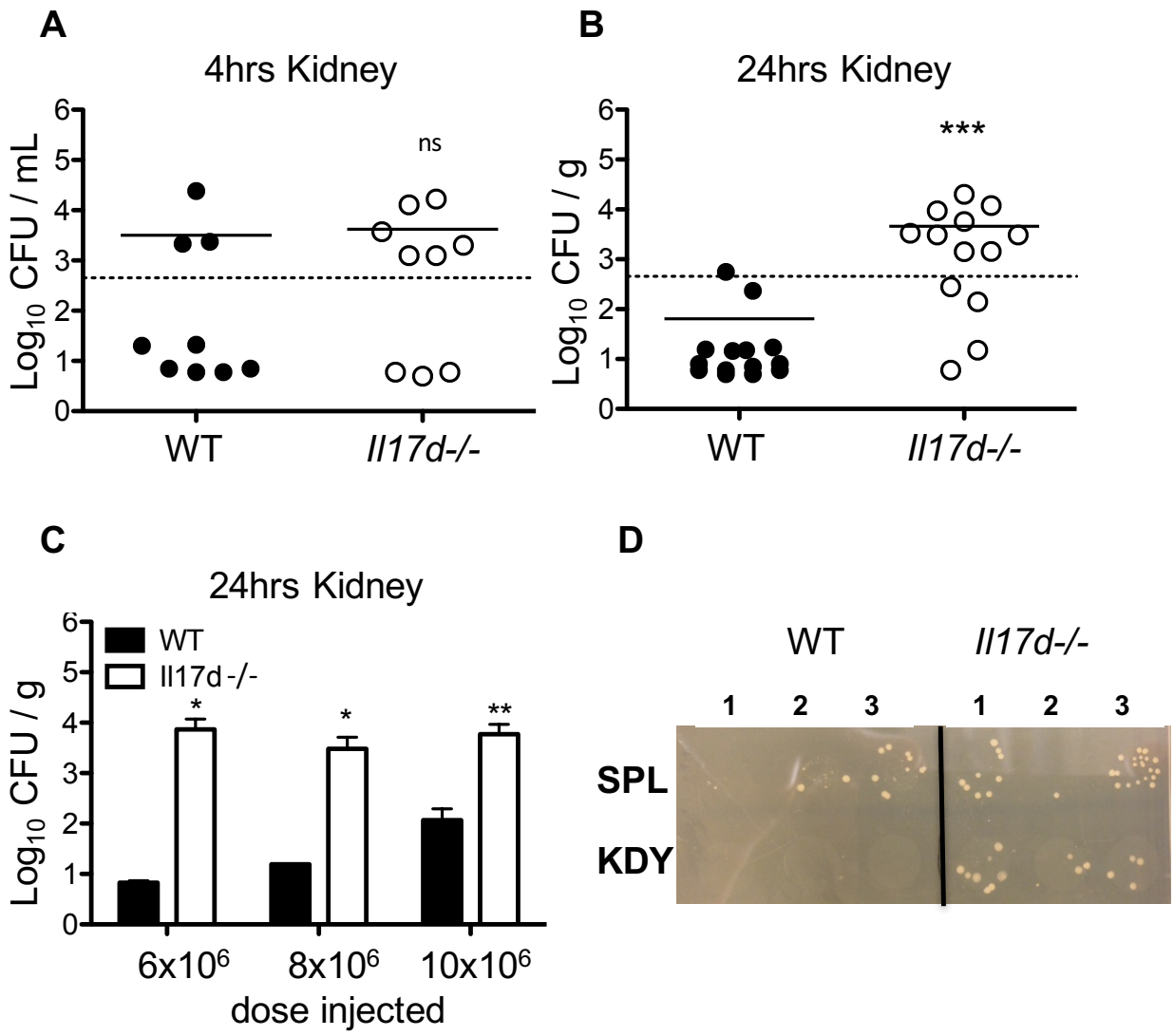

Figure 3.3 IL-17D knock-outs trends in higher renal bacterial burden compared to wild-type animal. (**A**) CFU of diluted kidney homogenate from 4 hours post-infected WT and Il17d-/- mice (i.p. $1x10^7$) and (**B**) bacterial burden from 24 hours post-infected mice. (**C**) CFU recovered in kidney after three separate increasing concentrations of i.p. GAS (24hr time point). (**D**) CFU of diluted organ (Spl, spleen; Kdy, kidney) homogenate from 24 hours post-infected mice (i.p. $1x10^7$). Data shown are mean only or mean ± SEM and are representative or combined data of at least 2-4 independent experiments. *, $P < 0.05$; **, $P < 0.01$; ***, $P < 0.001$.

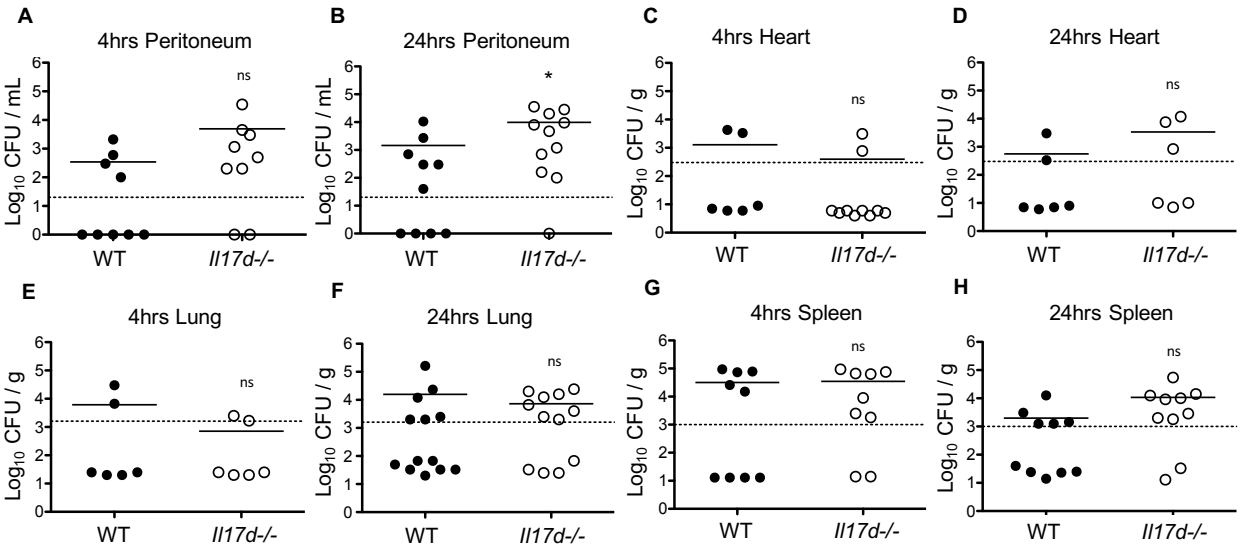

Figure 3.4 Peritoneal burden in Il17d-/- mice is higher than WT; Heart, lung, and spleen are not significantly different. (**A**) CFU recovered from peritoneum after 4hours or **(B)** 24 hours post-GAS infection in WT and Il17d-/- mice. (**C**) CFU recovered from heart homogenate after 4 hours or (**D**) 24 hours post-GAS infection. (**E**) CFU recovered from lung homogenate after 4 hours or (**F**) 24 hours post-GAS. (**G**) CFU recovered from spleen homogenate after 4 hours or (**H**) 24 hours (p=0.064) post-GAS. All GAS concentration for i.p. injection was $1x10^7$ cells per mice. Data shown are mean only and are representative or combined data of at least 2 independent experiments. *, $P < 0.05$

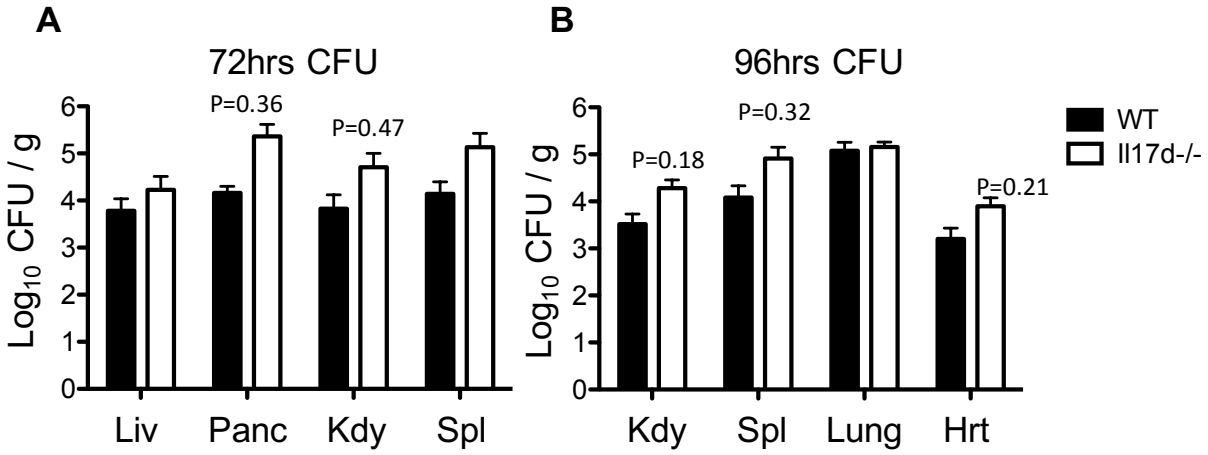

Figure 3.5 GAS burden in *Il17d*-/- mice is not significantly different to WT at days 3 and 4. (**A**) CFU recovered from liver (Liv), pancreas (Panc), kidney (Kdy), and spleen (Spl) after 72 hours post GAS infection. **(B)** CFU recovered from kidney, spleen, lung, and heart (Hrt) after 96 hours post GAS infection (i.p. $1x10^7$ cells per mice). Data shown are mean ± SEM and is a representative data of 2 independent experiments (n>3).

CHAPTER IV: INTERLEUKIN-17D INDUCES CCL2 AND MEDIATES IMMUNE RESPONSE AGAINST GROUP A STREPTOCOCCAL RENAL INFECTION

4.1 Introduction

Intraperitoneal injection of pathogens results in rapid recruitment of immune cells predominated by neutrophils and monocytes. Immune cells in inflammatory events are recruited as a result of expression of cytokines, such as the IL-17s, that are secreted at the infected site (14). We have previously found IL-17D to have a role in anti-tumor and anti-viral immunity via recruitment of NK cells via inducing pro-inflammatory effectors such as CCL2 (aka MCP-1) (6-10). In fact, *Il17d-/-* mice are thus more susceptible to viral infection and carcinogen-induced tumor, due to compromised immune cell recruitment to carry out surveillance (8, 9).

Starnes and colleagues have previously found relatively higher base line IL-17D expression in organs such as brain, muscle, heart, and kidney (16). Since we found higher bacterial burden in the kidney of Il17d-/- mice (Chapter III), we continued to focus our investigation on the role of IL-17D in renal infection by GAS. We hypothesized that IL-17D mediates early anti-bacterial immunity in part by inducing chemokines such as CCL2 and recruiting neutrophils into the infected site.

4.2 Results

4.2.1 IL-17D induces immune cell recruitment

In order to test whether IL-17D mediates immune cell recruitment in GAS infection, we utilized the peritoneal injection model in mice. We first observed that recombinant IL-17D i.p. injection induced *Ccl2* in the mesothelial tissue of the peritoneal cavity after 2 hours (**Fig. 4.1A**) and neutrophils are significantly higher in the peritoneum at 4 hours after IL-17D injection in WT and Rag-/- mice (**Fig. 4.1B, 4.1C**). In fact, intraperitoneal injection of IL-17D increased the

overall number of CD45+ peritoneal immune cells (**Fig. 4.2A**) by also increasing the presence of monocytes and macrophages in the peritoneum (**Fig. 4.2B, C**), which mirrors the effect of i.p. injection of IL-17A. At base line, we observed that $CD11b^{hi}$ cells predominate the peritoneal cavity of mice (**Fig. 4.3A-C**). However, after bacterial infection, Ly6g+ cells (neutrophils) predominated the peritoneal cavity (**Fig. 4.3D**).

4.2.2 Group A Streptococcal infection induces CCL2, IL-17D, recruits neutrophils

Since IL-17D can independently recruit neutrophils, we sought to answer whether bacterial infection induces IL-17D. We first confirmed that IL-17D is induced in the kidney after GAS infection (**Fig. 4.4A**). We next asked whether endogenous IL-17D induces *Ccl2* in some infected organs. Indeed, *Il17d*-/- kidney displayed ostensible decreases in *Ccl2* at 4 hour- and 24 hour- post GAS infection (**Fig. 4.4B**). Furthermore, although the baseline neutrophil content in the *Il17d*-/- mice is higher ($p<0.05$) than in WT kidney (**Fig. 4.4C**), there was a trend for lower neutrophil numbers ($p=0.31$) in GAS-infected *Il17d*-/- kidney (**Fig. 4.4D**). We separately confirmed the presence of neutrophils in the kidney and spleen infected by GAS via the intraperitoneal route (**Fig. 4.5A, 4.5B**). The observation of lower neutrophil is consistent with lower CD45+ cells ($p=0.06$) in *Il17d*-/- kidney after infection (**Fig. 4.6**). Chemokines such as cxcl1 and cxcl2 were not dependent upon IL-17D in GAS-infected kidney (**Fig. 4.7A, 4.7B**). The kidney injury molecule, which indicates damage to the organ, was not different in WT and Il17d-/- kidney infected by GAS (**Fig. 4.7C**). Contrary to data obtained for kidney, Ccl2 in spleen was not IL-17D-dependent (**Fig. 4.8A**). Similar to kidney, base line neutrophil numbers in the spleen and peritoneum were trending slightly higher in *Il17d*-/- mice, but did not differ from WT animals after GAS infection (**Fig. 4.8B, 4.8C, Fig. 4.9A, 4.9B**). Ccl2 in the peritoneal immune cells after infection was also lower in the *Il17d*-/- mice (**Fig. 4.9C, 4.9D**).

4.3 Discussion

We found a significant increase in *Il17d* and *Ccl2* upon in vivo GAS infection of the wild-type (WT) kidney and also detected a trend for lower neutrophil infiltration and relatively lower *Ccl2* transcript in the *Il17d*-/- kidney compared to WT. In our studies, the kidney demonstrated a relatively lower ratio of immune cells to non-immune cells, compared to organs such as lungs and spleen. As such, organs with relatively lower resident immune cells may depend more so on recruitment in the event of a local infection. We showed that recombinant IL-17D induces Ccl2 in vivo and also recruits neutrophils into the instilled site, which suggests *Il17d*-/- mice may be impaired in downstream chemokine production at certain sites. Since the kidney is relatively lower in resident immune cells compared to organs such as lung and spleen, we speculate that *Il17d*-/- mice may face greatest disadvantage in warding off bacterial infection in organs dependent on effective recruitment of actively responding innate immune cells. Impaired recruitment or perhaps the accompanying activation by lacking IL-17D at the infected sites thus translates into higher bacterial CFU we observed in *Il17d*-/- kidney homogenates. Our present study suggests a role for IL-17D in mammalian anti-bacterial immunity, whereby *Ccl2* is induced and neutrophil is recruited into lesions burdened with actively replicating bacteria, although it may be compensated for in certain tissues due to overlapping functions with other IL-17 cytokines.

Chapter IV, in full, is an adapted version of the material that has been prepared for publication. **Washington A Jr**, Varki N, Valderrama JA, Nizet V, Bui JD. IL-17D mediates anti-bacterial immunity in Group A Streptococcus infection. Manuscript in preparation. The dissertation author was the primary author of all material.

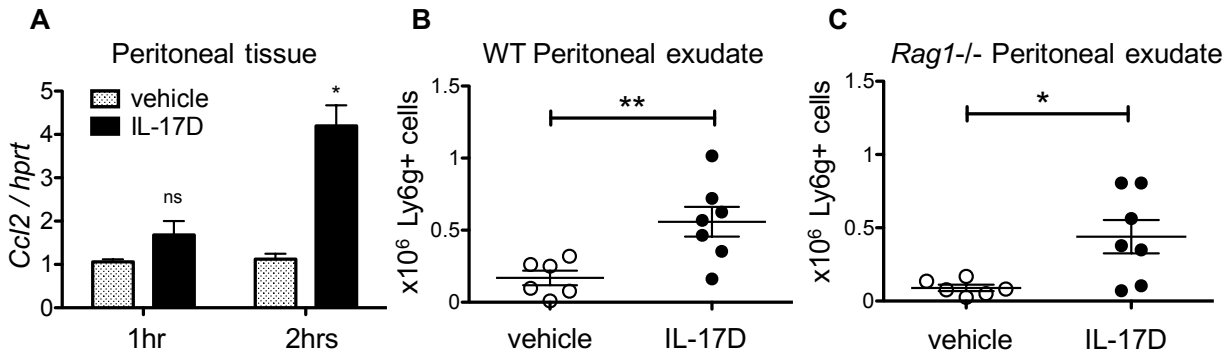

Figure 4.1 IL-17D induces Ccl2 and recruits neutrophils in the kidney of wild-type mice. (**A**) Relative *Ccl2* transcript in the peritoneal tissue after i.p. IL-17D injection; n=3. (**B**) Absolute neutrophil numbers in the peritoneum of wild-type and (**C**) *Rag-/-* mice post 4 hours i.p. IL-17D injection. Data shown are mean ± SEM and are representative or combined data of at least 2 independent experiments. *, $P < 0.05$; **, $P < 0.01$.

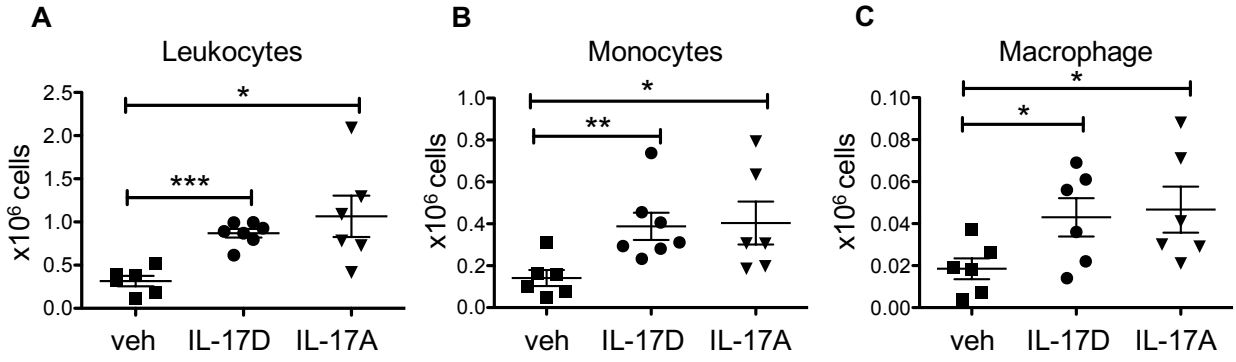

Figure 4.2 IL-17D and IL-17A similarly recruit monocytes and macrophages in the peritoneum. (**A**) Absolute number of CD45+ cells, (**B**) CD11b+ Ly6C+ monocytes, and (**C**) F4/80+ CD11b^{hi} macrophage in the peritoneal exudate after 4 hours i.p. cytokine (500ng) injection. Data shown are mean ± SEM and are representative or combined data of at least 3 independent experiments. *, $P < 0.05$; **, $P < 0.01$; ***, $P < 0.001$.

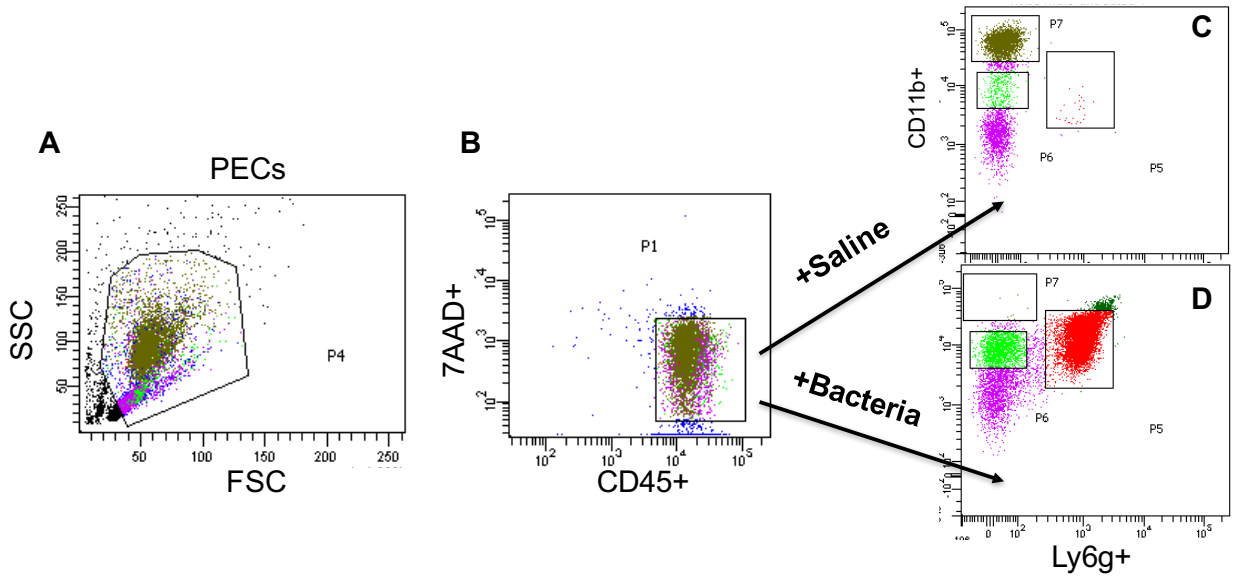

Figure 4.3 Neutrophils are first responders to bacterial infection in the peritoneum. (**A**) Representative image of peritoneal exudate cells (PECs) from 12 weeks old WT and Il17d-/- mice. (**B**) Gating strategy to capture viable (7AAD negative) peritoneal immune cells. (**C**) Gating strategy to capture neutrophil (Ly6g+ cells) after 24 hours PBS or (**D**) GAS i.p. injection.

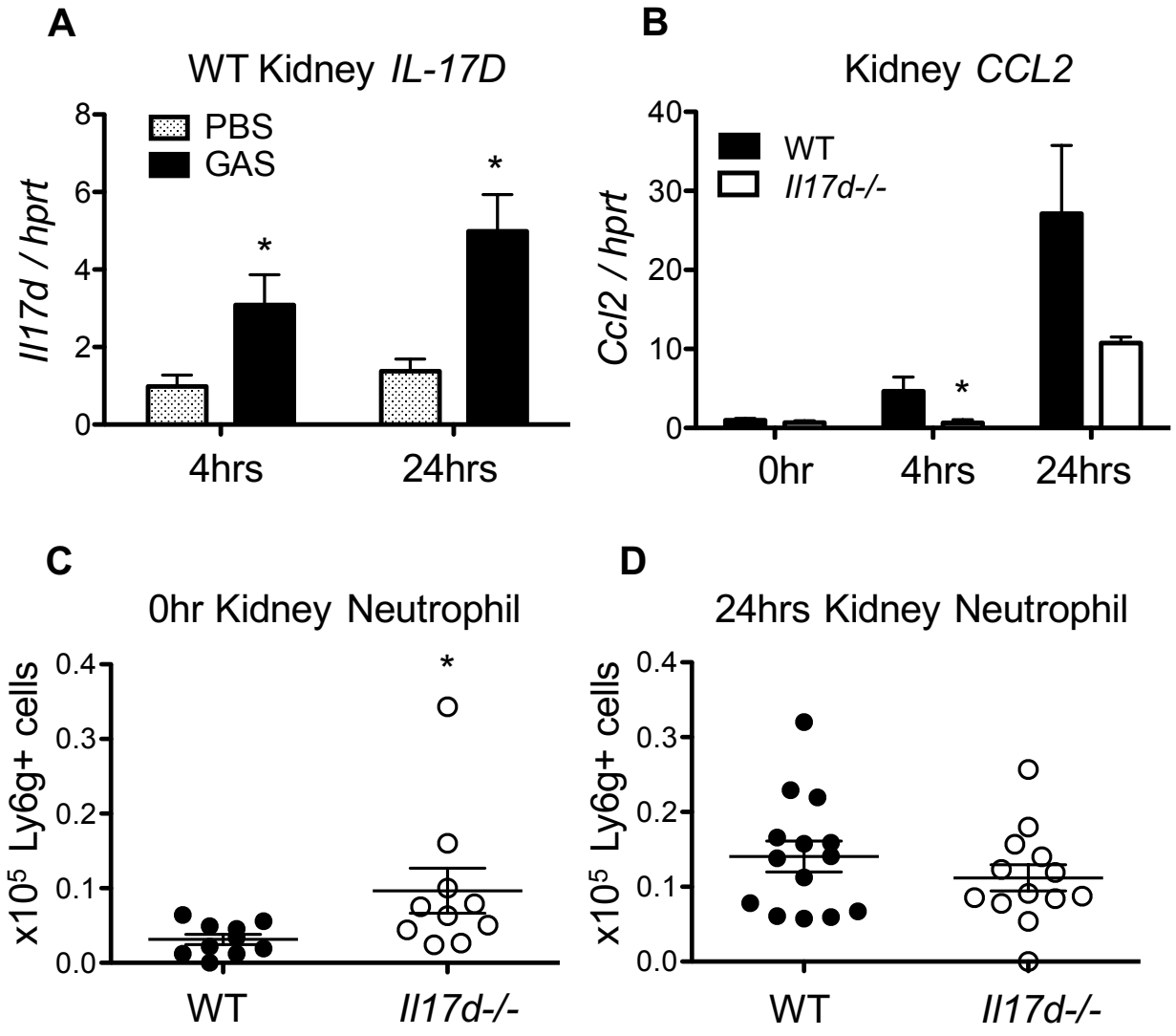

Figure 4.4 IL-17D and Ccl2 are induced and neutrophils are possibly recruited into the kidney of GAS-infected mice. (**A**) Relative *Il17d* transcript and (**B**) relative *Ccl2* transcript in the kidney homogenate after i.p. GAS infection. (**C**) Absolute number of renal neutrophils in uninfected ($p<0.05$) and (**D**) 24 hours post-infected mice ($p=0.31$). Data shown are mean ± SEM and are representative or combined data of at least 2-4 independent experiments. *, $P < 0.05$

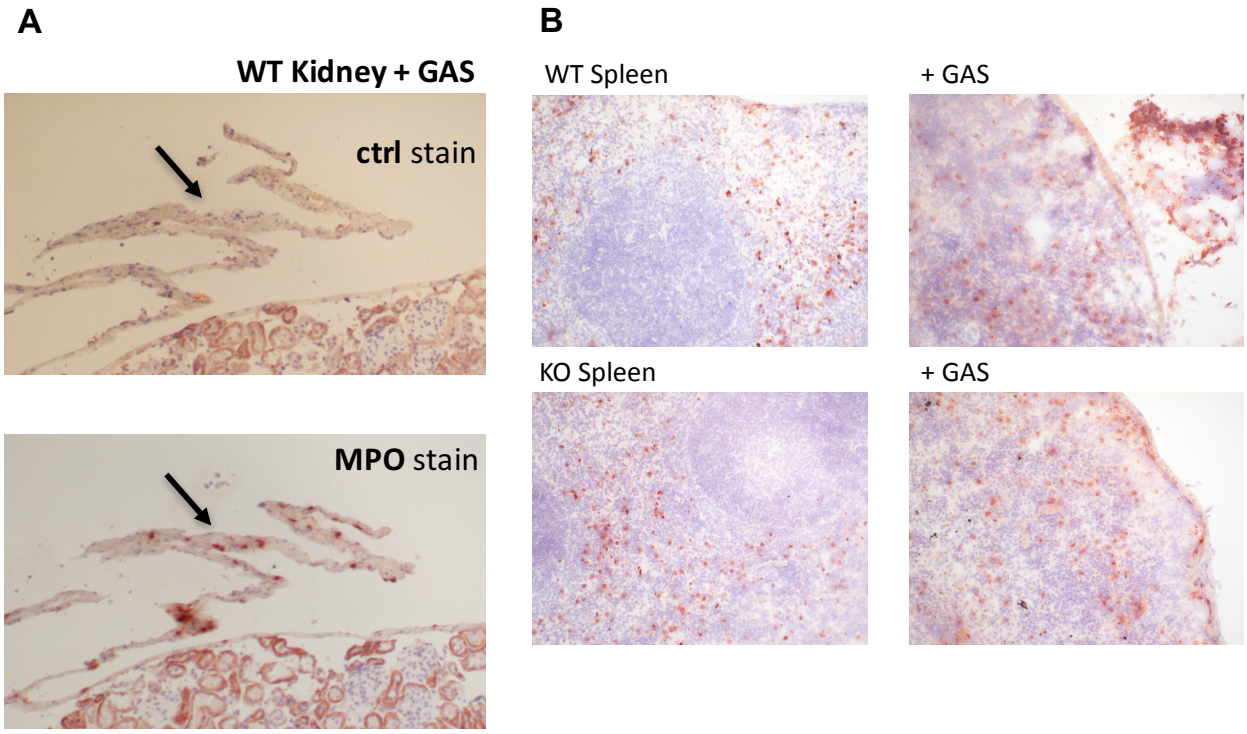

Figure 4.5 Neutrophils are recruited into kidney and spleen after i.p. GAS-infection. (**A**) Neutrophil myeloperoxidase (MPO) stain in kidney. (**B**) WT and *Il17d*-/- spleen from mice infected by GAS after 24 hours via i.p. injection. Representative images (n=4).

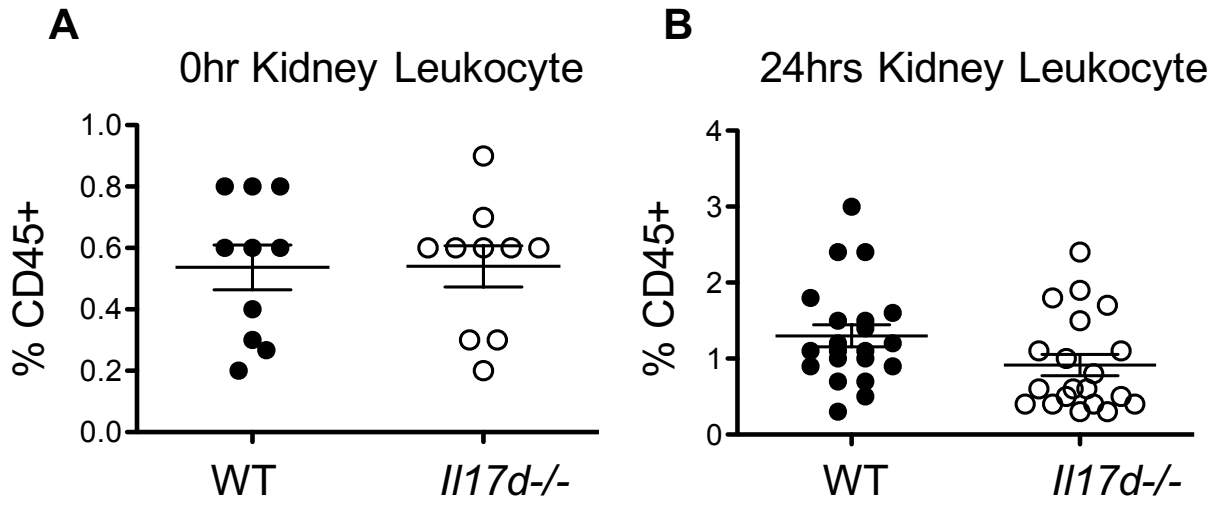

Figure 4.6 Percentage of renal immune cells is lower in GAS-infected *Il17d*-/- mice. (**A**) CD45 positive cell percentage in peritoneum at base line and (**B**) 24hrs post-GAS infection (p=0.06) in WT versus *Il17d*-/- mice. Data shown are mean and SEM and are representative data of at least 2 independent experiments. *, $P < 0.05$

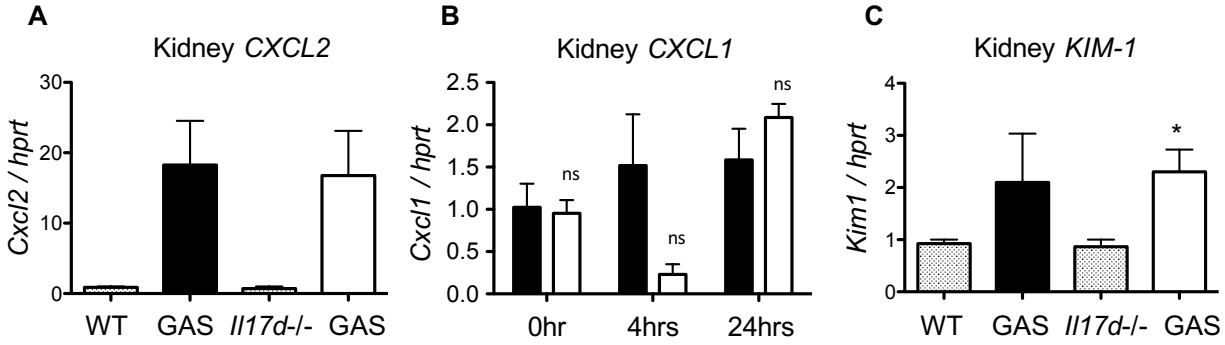

Figure 4.7 Renal Cxcl1, Cxcl2, and tissue damage is unaffected in *Il17d*-/- mice. (**A**) Cxcl2 transcript and (**B**) Cxcl1 transcript measured in kidney after GAS infection ($1x10^7$ i.p.). (**C**) Kidney injury molecule, Kim-1, measured after 24 hours GAS infection. Data shown are mean ± SEM and are representative data of at least 2 independent experiments. *, $P < 0.05$

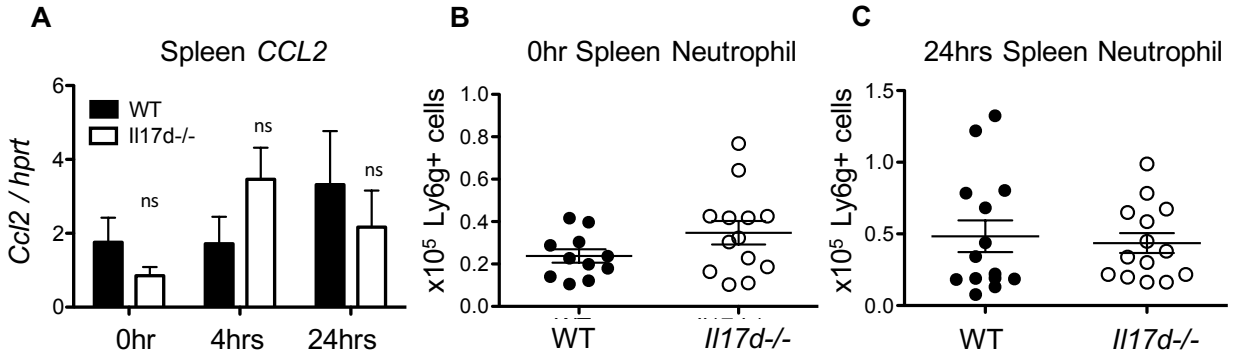

Figure 4.8 Neutrophil content and Ccl2 in spleen are unaffected in *Il17d*-/- mice. (**A**) Peritoneal exudate cells from 12 weeks old WT and Il17d-/- mice (n=4). (**B**) Absolute number of peritoneal neutrophils at base line (p=0.12) or (**C**) 24 hours (p=0.72) post-GAS infection ($1x10^7$ i.p.). Data shown are mean ± SEM and are representative data of at least 2 independent experiments. *, $P < 0.05$

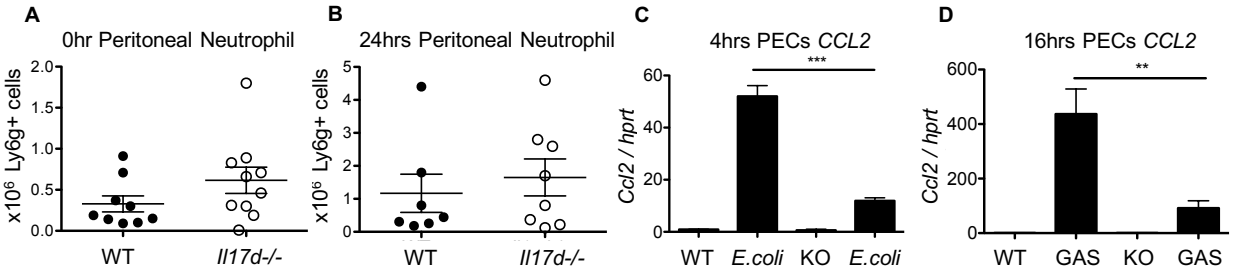

Figure 4.9 *Ccl2* transcript in peritoneal cells is lower in *Il17d*-/- mice infected by bacteria. (**A**) Peritoneal exudate cells from 12 weeks old WT and Il17d-/- mice. (**A**) Absolute number of peritoneal neutrophils at base line or (**B**) 24 hours post-GAS infection ($1x10^7$ i.p.). (**C**) Relative Ccl2 transcript in the peritoneal exudate cells (PECs) from 12 weeks old WT and *Il17d*-/- mice after 4hours i.p. *E.coli* infection, or (**D**) 16hrs i.p. GAS infection ($1x10^7$). Data shown are mean ± SEM and are representative data of at least 2 independent experiments. **, P <0.01; ***, P < 0.001.

Table 4.1 List of primers for qPCR

Name	Sequence (5' to 3')
MOUSE	
Gapdh (forward)	GAACGGGAAGCTCACTGGCATGGCC
Gapdh (reverse)	TGTCATACCAGGAAATGAGCTTGAC
Hprt (forward)	GCTTGCTGGTGAAAAGGACCTCTCGAAG
Hprt (reverse)	CCCTGAAGTACTCATTATAGTCAAGGGCAT
Il17d (forward)	AGCTTGTCCATGCTGGAGTT
Il17d (reverse)	CTCTACGGGGAGGAGGACTT
Dct (forward)	TTCGCAAAGGCTATGCGC
Dct (reverse)	GTTACTACCCAGGTCAGGCCAG
Pax3 (forward)	AACCCACTACCCAGACATTTAC
Pax3 (reverse)	CCAGCTTGTTTCCTCCATCT
Sox10 (forward)	CAGGTGTGGCTCTGCCCACG
Sox10 (reverse)	GTGTAGAGGGGCCGCTGGGA
Kim1 (forward)	CATATCGTGGAATCACAACGAC
Kim1 (reverse)	ACAAGCAGAAGATGGGCATTG
Ccl2 (forward)	TAAAAACCTGGATCGGAACCAAA
Ccl2 (reverse)	GCATTAGCTTCAGATTTACGGGT
Il6 (forward)	AGCCAGAGTCCTTCAGAGAGATAC
Il6 (reverse)	TCTTGGTCCTTAGCCACTCCTTC
RAT	
Gapdh (forward)	AGACAGCCGCATCTTCTTGT
Gapdh (reverse)	CTTGCCGTGGGTAGAGTCAT
Il6 (forward)	TCTCTCCGCAAGAGACTTCCA
Il6 (reverse)	ATACTGGTCTGTTGTGGGTGG
HUMAN	
Gapdh (forward)	ACCCACTCCTCCACCTTTGA
Gapdh (reverse)	CTGTTGCTGTAGCCAAATTCGT
Hprt (forward)	CAAGCTTGCTGGTGAAAAGGAC
Hprt (reverse)	GTCAAGGGCATATCCTACAACAAA
Il17d (forward)	TGGGCCTACAGAATCTCCTACGACC
Il17d (reverse)	TGACGTAGGCCTCGGTGTAGACGG

CHAPTER V: VIABLE GROUP A STREPTOCOCCUS INDUCES OXIDATIVE STRESS-MEDIATED INTERLEUKIN-17D EXPRESSION

5.1 Introduction

In order to mount swift action to fight off pathogens, cells recognize the pathogen-associated molecular patterns (PAMPs) through pattern recognition receptors (PRRs), triggering a panoply of responses and signaling pathways including for some PRRs the production of reactive oxygen species (ROS) and cytokines (45). Matzinger further stipulated the distinction of PAMPs as harmless versus harmful in dictating the degree of inflammation warranted (46). However, it is currently unclear whether cells respond to pathogen viability: that is, by discriminating whether the organism is alive or dead. Indeed, at least for immune cells, increasing evidence point to demonstrable distinction between PAMPs produced by the living versus the dead, such as RNA and c-di-AMP (47-49). Furthermore, attenuated ROS production has been observed in epithelial cells infected by adhesion-incompetent or heat-killed GAS (50-52). The effect of viable pathogen on cytokine production in non-immune cells remains unresolved.

Cytokines IL-17A and IL-17F are positively regulated in CD4+ T cells by retinoic acid-related orphan nuclear receptor, RORγt and RORα (53-55). Although transcriptional regulation remains unclear for IL-17C, it is induced in response to extracellular Gram-negative bacteria in epithelial cells (24, 56). Similarly, IL-17E in epithelial cells is induced upon detecting extracellular helminth and its metabolite, succinate (57, 58). IL-17D has been found to be positively regulated by viral infection and anti-oxidant factor Nrf2 (8-10). Although bacterial infection by species such as GAS generates ROS (50, 51), it is not known whether and how IL-17D is induced in response to GAS infection.

5.2 Results

5.2.1 Viable Group A Streptococcus induces IL-17D in non-immune cells.

In order to determine in which cells IL-17D is induced, we performed a brief in vitro infection of peritoneal exudate cells versus several epithelial cell lines of mouse and human origin. A GAS-to-host ratio of 1:1 was sufficient to elicit increase in *Il17d* transcript in non-immune cells, including primary renal cells (**Fig. 5.1A, 5.1B, 5.1C**). We did not detect increase in *Il17d* transcript in some primary cells from organs such as lung and spleen (**Fig. 5.2**). Since Valderrama and colleagues demonstrated the importance of M1 cell surface protein of GAS in IL-1β production in macrophage (59), we tested the ability of M1 deficient GAS in inducing IL-17D. We did not observe difference in *Il17d* transcript or IL-17D protein in non-immune cells infected by wt GAS versus m1Δ GAS (**Fig. 5.3**). However, to our surprise, inducing *Il17d* in non-immune cells was compromised when the bacteria were heat-killed (**Fig. 5.4A**). On the other hand, viability of GAS did not affect the induction of *Il17d* in immune cells (**Fig. 5.4B**). We also confirmed that non-immune cells had higher *Il17d* when another bacterial species (*E. coli*) was alive versus dead (**Fig. 5.4C**). Since viable bacteria can divide during the course of the experiment, there could be quantitative differences in total exposure of cells to live versus dead bacteria. Therefore, we next asked whether adjusting for final GAS number in medium would account for the difference. We determined viable GAS would be 3-4 fold higher in number as a result of replication in the assay medium after 3 hours (not shown). Diluting the infection ratio to account for replication, we confirmed that living GAS was still able to induce *Il17d* more so than incubation with the dead GAS when total bacterial burden was taken into account (**Fig. 5.4D, Fig.5.4E**), while *Tnfa* was induced according to bacteria quantity, irrespective of viability (**Fig. 5.4F**). We also confirmed that peptidoglycan alone did not induce *Il17d* (**Fig. 5.5A**). In this

experiment, we observed *Tnfa* increase after peptidoglycan treatment or incubation with heat-killed GAS (**Fig. 5.5B**).

5.2.2 Group A Streptococcus infection induces IL-17D.

Conversely, we also confirmed that viable bacteria could induce higher *Il17d* than heat-killed GAS at a higher multiplicity of infection ratio (**Fig. 5.6A**). Since living GAS is able to cause ROS production, we tested to see whether treating the infected cells with ROS scavenger attenuates the induced levels of IL-17D. We confirmed that IL-17D is induced in epithelial cells infected by live GAS, while two different ROS scavengers independently abrogated the effect (**Fig. 5.6B**). At this early time point, ROS scavengers themselves did not yet have an inhibitory effect on the growth of GAS in the assay medium (**Fig. 5.6C**).

5.3 Discussion

We have previously reported that oxidative stress can lead to IL-17D expression via the activation of the antioxidant transcription factor, *Nrf2* (8-10). Oxidative stress is caused by GAS invasion-triggered caspases and ROS production and is linked with cell death and pro-inflammatory events in macrophages and epithelial cells (45, 50, 51, 59). Since incubation with heat-killed GAS fails to induce the production of ROS, we speculated that some ROS-dependent cytokines such as IL-17D fail to be induced without active invasion by GAS. In fact, previous studies have reported on the elusive nature of pinpointing bonafide GAS ligands for host TLR (60-62). Our data did not find extracellular components of GAS such as M1 protein or peptidoglycan to be responsible for inducing IL-17D. Our current findings suggest that cytokines such as IL-17D are regulated in part through detecting the viability of the infectious agent, aside from TLR. Further research is required to determine whether there are other cytokines or defense arsenals that are regulated through detection of infectious danger posed by living pathogens.

Chapter V, in full, is an adapted version of the material that has been prepared for publication. **Washington A Jr**, Varki N, Valderrama JA, Nizet V, Bui JD. IL-17D mediates anti-bacterial immunity in Group A Streptococcus infection. Manuscript in preparation. The dissertation author was the primary author of all material.

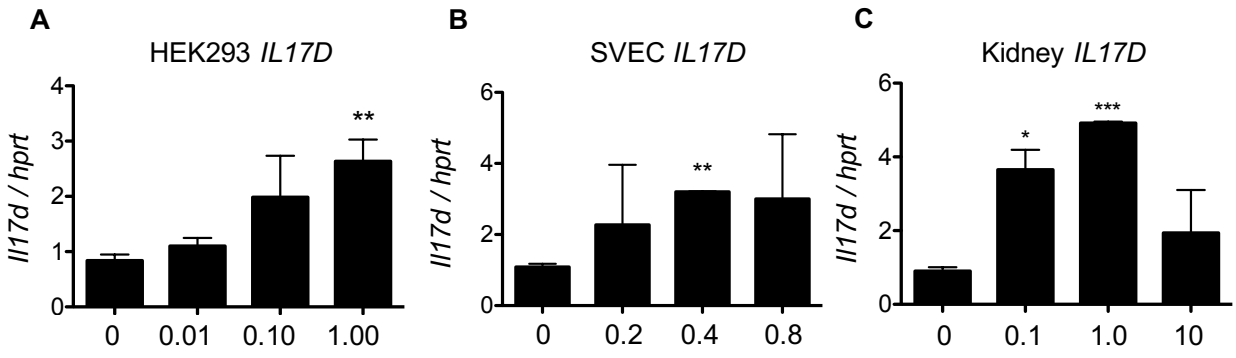

Figure 5.1 IL-17D is induced by GAS in vitro. (**A**) Epithelial cells (HEK293), (**B**) endothelial cells (SVEC), and (**C**) kidney homogenate cells were cultured in vitro and incubated with GAS at indicated MOI for 3 hours (n=3). Data shown are mean ± SEM and are representative data of at least 3 independent experiments. *, $P < 0.05$; **, $P < 0.01$; ***, $P < 0.001$.

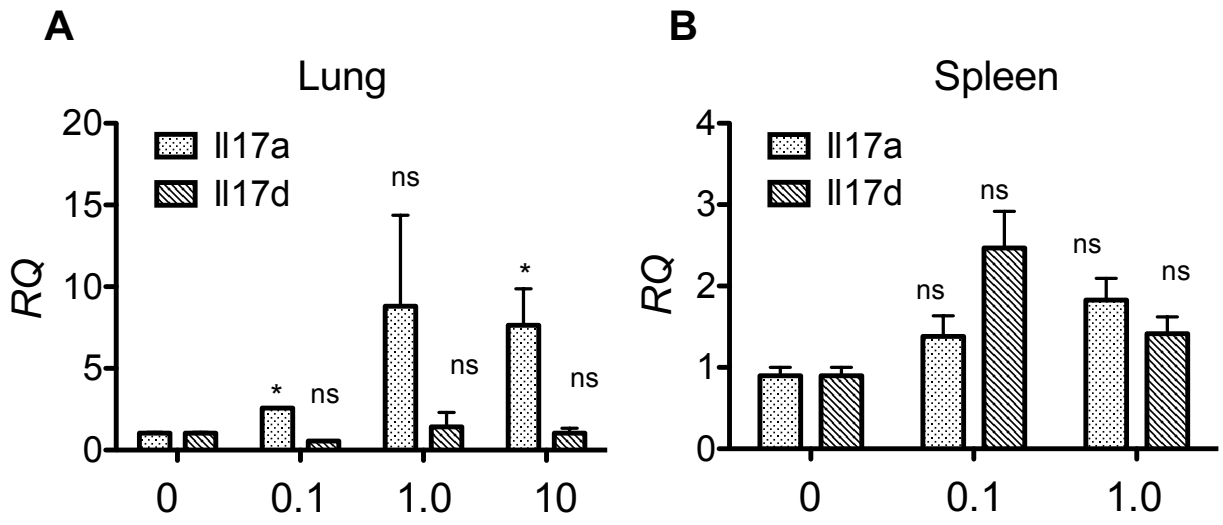

Figure 5.2 IL-17D is not induced in GAS-infected cultured cells from lung or spleen. (**A**) Lung homogenates were cultured in vitro and incubated with GAS at indicated MOI for 3 hours. **(B)** Spleen homogenates were cultured in vitro and incubated with GAS at indicated MOI for 3 hours. Data shown are mean ± SEM and are representative data of at least 3 independent experiments. *, $P < 0.05$

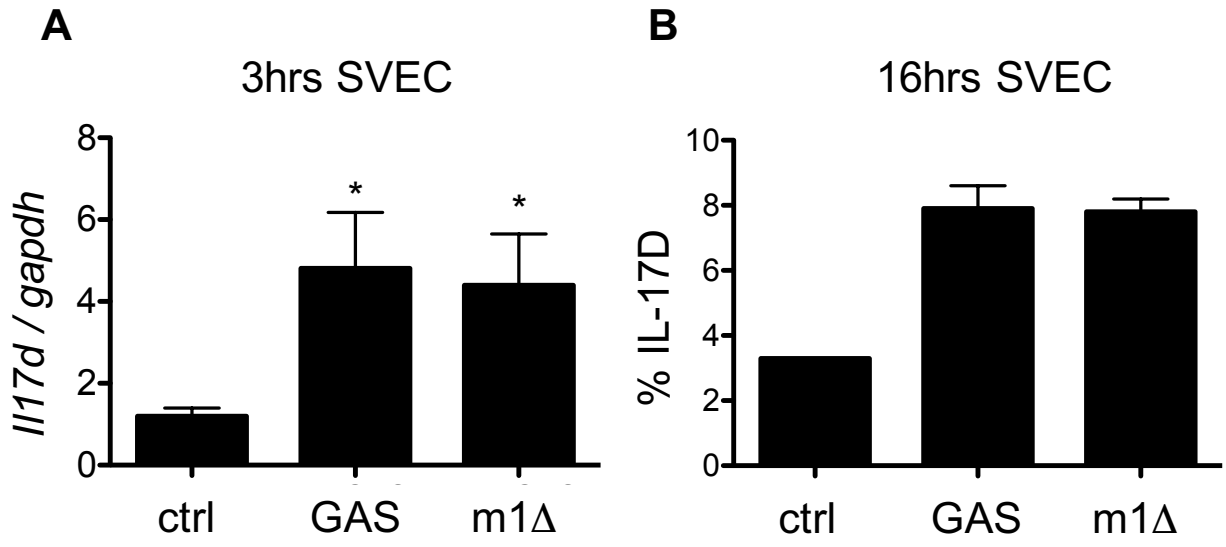

Figure 5.3 GAS M1 protein is dispensable to induce IL-17D in vitro. (**A**) Relative Il17d transcript in endothelial cells (SVEC) after 3 hours and (**B**) intracellular protein IL-17D detected after 16 hours in culture post-GAS infection. Data shown are mean ± SEM and are representative data of at least 3 independent experiments. *, $P < 0.05$

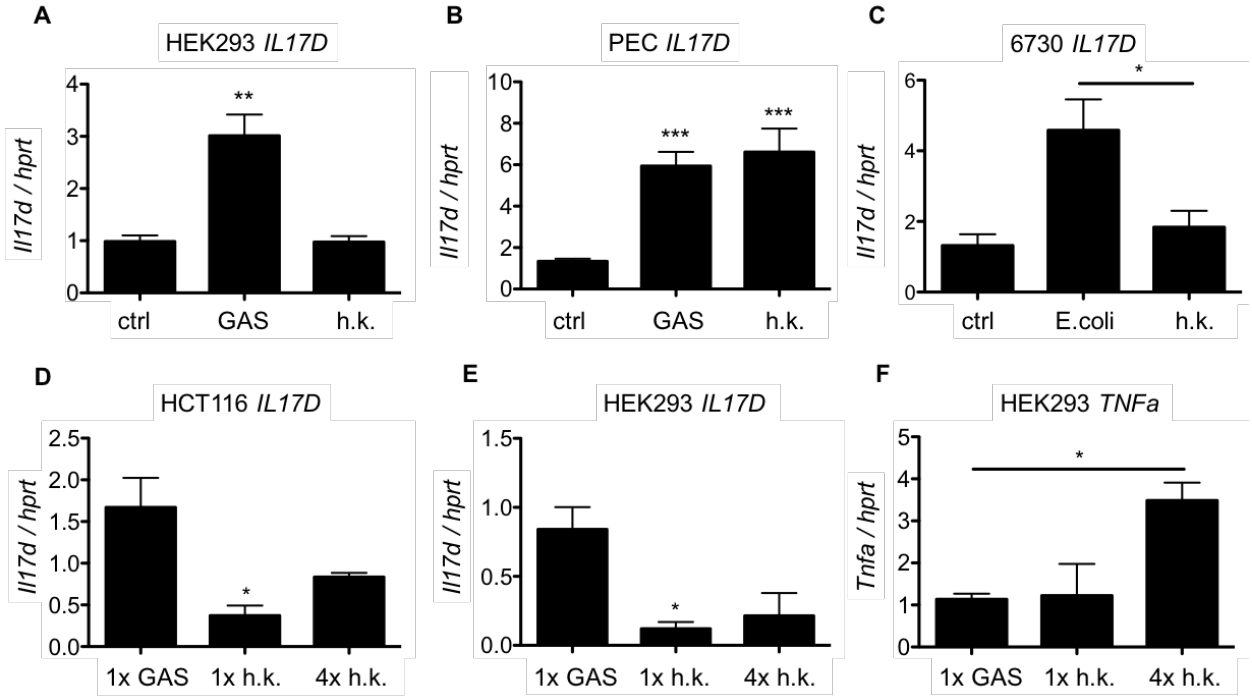

Figure 5.4 IL-17D is induced by viable GAS in epithelial cells. (**A**) Epithelial cells (HEK293) and (**B**) peritoneal exudate cells (PECs) were cultured in vitro and incubated with viable GAS or heat-killed (h.k.) GAS for 2 hours. (**C**) Mouse sarcoma cells were cultured with viable E.coli or heat-killed E.coli for 3 hours. (**D**) Relative Il17d transcript in colon carcinoma cells and (**E**) HEK cells after 2 hours of GAS incubation. (**F**) Relative Tnfa transcript in HEK cells. Living GAS or heat-killed GAS incubated at 1:1 ratio unless indicated otherwise. Data shown are mean and SEM and are representative data of at least 3 independent experiments. *, $P < 0.05$; **, $P < 0.01$; ***, $P < 0.001$.

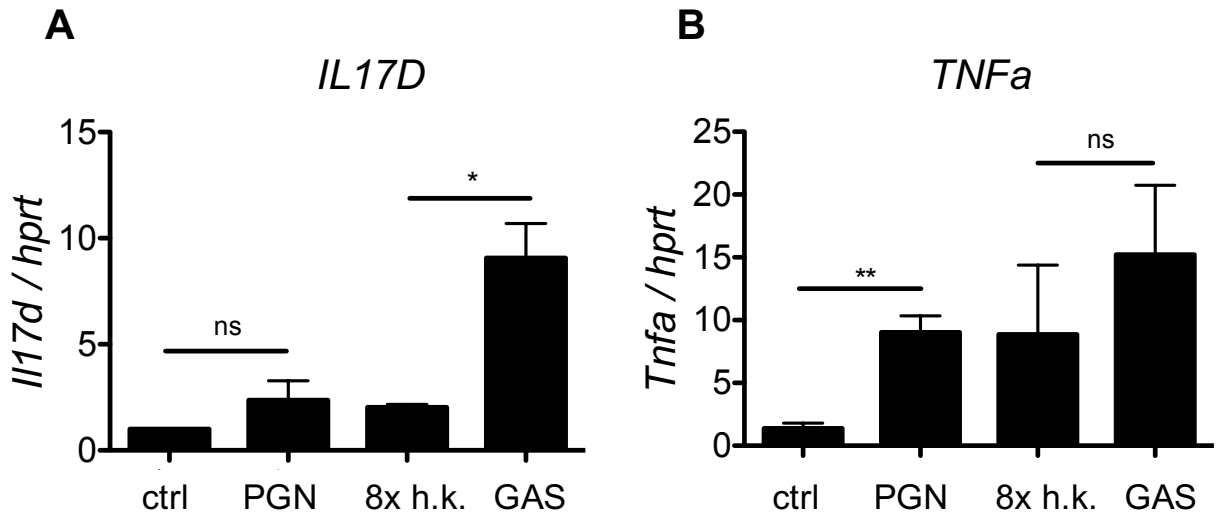

Figure 5.5 IL-17D is not induced by IL-17D. (**A**) Relative Il17d and (**B**) tnfa in HEK293 cells after 2-hour incubation with peptidoglycan (PGN, 1ug/mL), heat-killed (h.k., 8:1) or viable GAS (1:1). Data shown are mean and SEM and are representative data of at least 3 independent experiments. *, $P < 0.05$; **, $P < 0.01$.

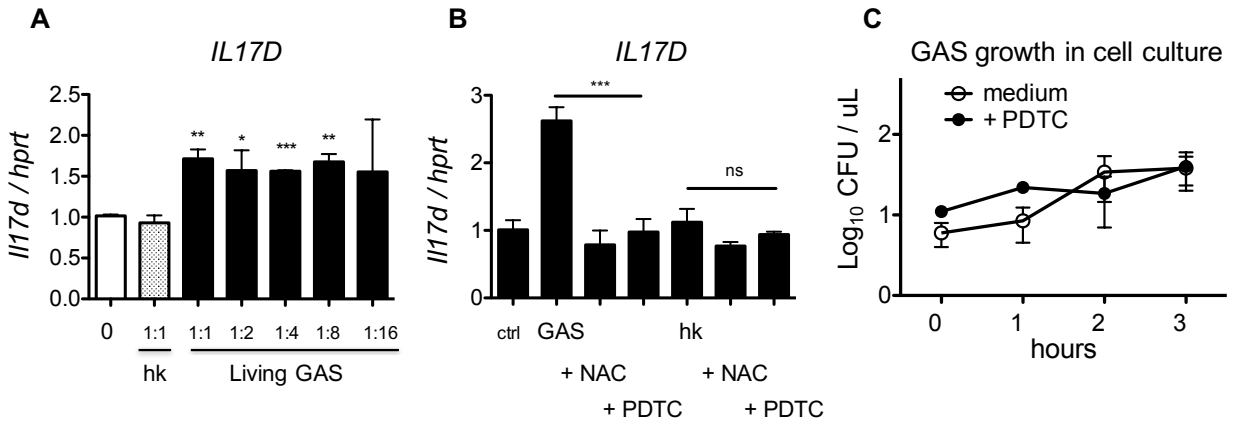

Figure 5.6 Reactive oxygen species production in GAS-infected cells induces IL-17D. (**A**) Relative *Il17d* transcript in HEK293 cells incubated with serially diluted viable GAS versus heat-killed (hk) GAS for 3hours. (**B**) Relative *Il17d* transcript in HEK293 cells pre-treated with ROS scavengers (NAC and PDTC) prior to co-incubation with viable or dead GAS. (**C**) Growth of GAS in cell culture medium (2% FBS) with and without ROS scavenger PDTC. Data shown are mean and SEM and are representative data of at least 3 independent experiments. *, $P < 0.05$; **, $P < 0.01$; ***, $P < 0.001$.

CHAPTER VI: HIGHER FREQUENCY OF DERMATITIS IN AGING MICE IN ABSENCE OF INTERLEUKIN-17D

6.1 Introduction

Ulcerative dermatitis is a debilitating condition, which approximately 4-20% aged C57BL/6 strain mice develop. Although the exact etiology is unknown, some of the known factors that predispose disease onset have been attributed to sex, diet, environment, and season (63). Lesions are typically acquired through pruiritus-induced self-injury, and further progress into ulcerations. The oxidative stress response of the dermatitic skin is normal, and is similar to that of a response in a wounded skin (64). However, Kastenmayer and colleagues have found that 50% of the mice deficient in inducible nitric oxide synthase (iNOS) gene developed dermatitis in a retrospective study (65).

Interleukin (IL)-17D is a cytokine in the IL-17 family that is broadly expressed in various tissues (16), and promotes immune responses to transformed or infected cells in part by inducing chemokines that recruit natural killer cells and neutrophils (6-10). Contrary to this pro-inflammatory role of IL-17D, we have also discovered a potentially anti-inflammatory function of IL-17D by observing increased incidence of dorsal dermatitis in aging *Il17d*-/- mice compared to wild-type (WT) mice. In order to investigate the underlying pathology, we sought to investigate the organs and tissues of aging *Il17d*-/- and WT mice with and without dermatitis.

6.2 Results

6.2.1 Aging IL-17D knockout mice have higher incidence of dermatitis.

Although IL-17D promotes pro-inflammatory immunity to defend against tumors and viral infections (6-10), an anti-inflammatory role for IL-17D has not been described. Here, we observed significantly higher incidence of ulcerative dermatitis in mice lacking IL-17D (**Fig.**

6.1A). Most pathology manifest in the dorsal scapular regions (**Fig. 6.1B**) by 18 months from date of birth in *Il17d*-/- mice.

6.2.2 Blood of aging Il17d-/- mice have higher basophil.

We hypothesized that the higher incidence of dermatitis may be explained in part by unbalanced chronic inflammation. Therefore, we examined the blood white blood cell (WBC) composition of WT versus *Il17d*-/- mice before the expected age of dermatitis development. In the blood of pre-dermatitic *Il17d*-/- mice (>10 months old; <20 months old), we observed higher percentage of basophils (p=0.03) and eosinophils (p=0.09) compared to age- and sex-matched WT mice (**Fig. 6.2A, 6.2B**). Absolute numbers of basophils (p=0.13) and eosinophils (p=0.054) were also noticeably higher in the *Il17d*-/- mice than in WT mice (**Fig. 6.2C, 6.2D**). We did not detect any difference in other immune cell numbers in the blood (**Fig. 6.3A**), and RBC values were in line with WT controls (**Fig. 6.3B**).

6.2.3 Inflammatory cells infiltrate aging Il17d-/- skin and pancreas.

We investigated the lesion caused by dermatitis in the Il17d-/- mice to confirm infiltration by immune cells. Indeed, compared to the normal contralateral tissues taken from scapular regions of *Il17d*-/- mice, inflamed lesions exhibited epidermal thickening and abound in neutrophils (**Fig. 6.4A-D**). In some cases, hyperkeratosis is very evident, with noticeable presence of mast cells in skin lesions (**Fig. 6.4E, 6.4F**). Since we previously observed that *Il17d*-/- mice manifest higher viral and bacterial burden in some organs after MCMV and GAS infection (9, **Fig. 3.3, Fig. 3.4**), we hypothesized that some organs other than skin would also exhibit pathological inflammation in the absence of IL-17D. Examining the tissue sections of 300-600 days old pre-dermatitic mice, we found that some organs in *Il17d*-/- mice such as the

pancreas had higher incidence of inflammation near the islet cells, compared to WT (**Fig. 6.5A-F**).

6.2.4 Higher body weight and peritoneal cells in pre-dermatitic Il17d-/- mice.

Peritoneal exudate cell (PEC) numbers were higher in particular in 12 weeks old male *Il17d*-/- mice ($p<0.01$) compared to WT mice (**Fig. 6.6A**), although absolute numbers of PECs in female *Il17d*-/- mice were similar to WT (**Fig. 6.6B**). We also found the body weight of male ($p<0.001$) and female ($p<0.05$) *Il17d*-/- mice to be higher compared to WT animals at both young (12 weeks old, **Fig. 6.6C, 6.6D**) and old (12 months old, **Fig. 6.6E**) ages. Interestingly, body weight of mice older than 13 months were similar between WT and *Il17d*-/- mice (**Fig. 6.6F**). We also conducted a comprehensive metabolic panel blood samples from *Il17d*-/- mice and found the values to be similar to matched WT mice (**Fig. 6.7**).

6.3 Discussion

In this study, we demonstrated that *Il17d*-/- mice are more prone to increased dermatitis and have higher basophils in the blood, in addition to higher inflammation in certain organs such as the pancreas. Dermatitis was observed only in mice at least one-year-old, which suggest the pathology to be largely dependent on age. The trend in higher percentage and number of basophil and eosinophil suggests elevated susceptibility of *Il17d*-/- mice to chronic allergic inflammation (CAI). Basophils are often sited in allergic inflammation, and indeed are capable of promoting CAI independently of mast cells and T cells (66). In fact, inflammatory events such as IgE-mediated chronic allergic dermatitis are initiated by basophils, even though this cell type represent only about 0.5% of immune cells in the peripheral blood (67). Whereas basophils are characterized as initiators of allergic inflammation, eosinophils have been characterized as the effectors that promotes and sustains IgE-mediated CAI (68). Our observation of higher incidence

of dermatitis in *Il17d*-/- mice therefore suggests a heretofore-underappreciated role of IL-17D in chronic inflammation.

We have previously determined the upstream regulator of IL-17D as Nrf2, a well-characterized anti-oxidant regulator (8). Although Nrf2 is mostly known for its anti-inflammatory role by inhibiting production of pro-inflammatory cytokines, we found Nrf2 required for inducing IL-17D (8, 9). In fact, our observation of increased dermatitis in *Il17d*-/- mice may be linked to Nrf2 because *Nrf2*-/- mice develop age-dependent inflammatory lesions and autoimmunity (22, 23). Additionally, recent reports on IL-17D by Lee and colleagues found enhanced CD8 T cell function post-Listeria infection in *Il17d*-/- mice, implicating IL-17D to also have anti-inflammatory functions (44). Together, these observations pave a more nuanced understanding of IL-17D's activities as mediating both pro- and anti-inflammatory processes. Subsequent chapters following this story will need to define the cell types that produce IL-17D and the physiological signals that provoke its expression in the skin and organs such as the pancreas.

Aging of the body, and consequently the immune system, increases susceptibility to infection, autoimmunity, and impairment of wound healing (69). In fact, increased incidence of inflammation near the islet in the pancreas and ostensible skin pathology we see in *Il17d*-/- mice is generally expected at an advanced age. Therefore, the higher frequency of pathology we observe in *Il17d*-/- mice compared to aging WT suggests a homeostatic role for IL-17D to balance the necessary versus pathologic inflammation. As we found IL-17D to induce potentially anti-inflammatory melanosome-associated genes in Chapter II, there may be differing and counterbalanced activities of IL-17D that is dictated by specific tissue and microenvironment cues leading to augmented or attenuated inflammatory responses.

Chapter VI is an adapted version of the material that has been prepared for publication. **Washington AJr**, Seelige R, Wilbur R, Varki N, Bui JD. Spontaneous ulcerative dermatitis in aging IL-17D knockout mice. The dissertation author was the primary author of all material.

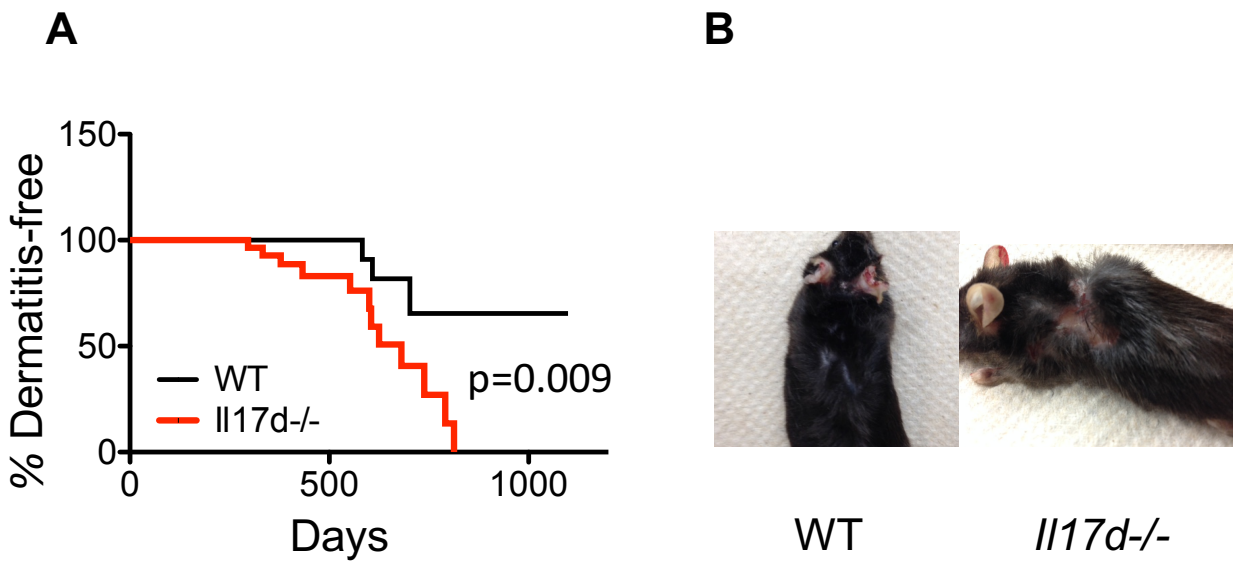

Figure 6.1 Aging Il17d-/- mice have higher dermatitis rate compared to wild-type animal. (**A**) Survey of aging wild-type C57BL/6 (WT) and Il17d-/- mice for development of dermatitis (n>30). (**B**) Representative image of mice with scapular dermatitis in WT and *Il17d-/-* mice over 600 days old.

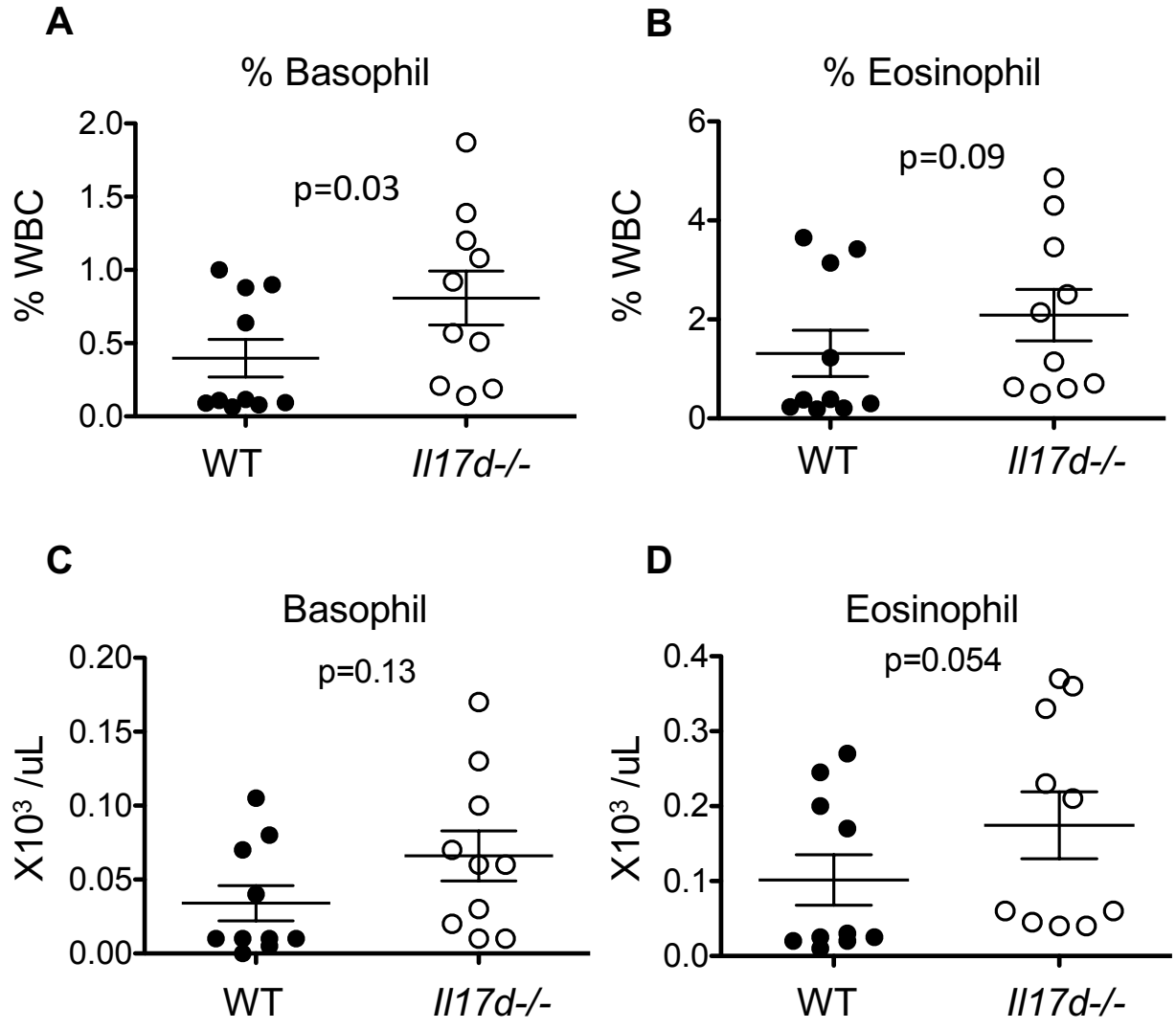

Figure 6.2 Aging Il17d-/- mice have higher basophil and eosinophil in peripheral blood. (**A**) Percentage of basophil or (**B**) eosinophil in white blood cells (WBC) from pre-dermatitic WT and *Il17d-/-* blood (from mice 300-600 days old). (**C**) Absolute number of basophil or (**D**) eosinophil in blood of aging pre-dermatitic mice (n=10). Data shown are mean ± SEM.

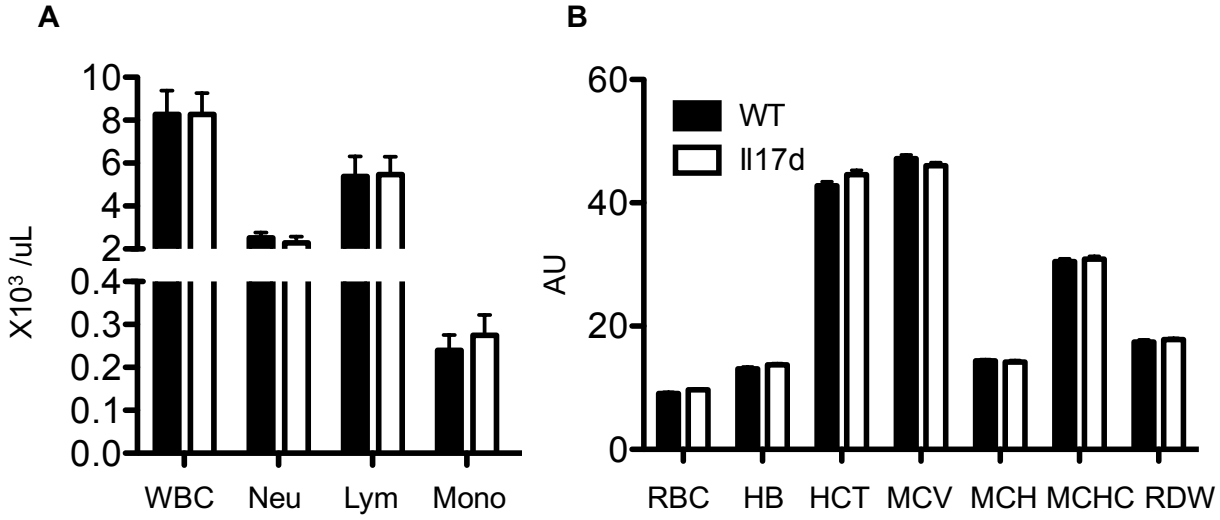

Figure 6.3 WBC and RBC measurements are similar to WT in aging *Il17d*-/- blood. (**A**) Complete blood count of white blood cells (WBC), neutrophils (Neu), lymphocytes (Lym), and monocytes (Mono). (**B**) Arbitrary units comparing values for red blood cell (RBC), hemoglobin (HB), hematocrit (HCT), mean corpuscular volume (MCV), mean corpuscular hemoglobin (MCH), mean corpuscular hemoglobin concentration (MCHC), and red blood cell distribution width (RDW) from pre-dermatitic WT and *Il17d-/-* blood (from mice 300-600 days old, n=10). Data shown are mean ± SEM.

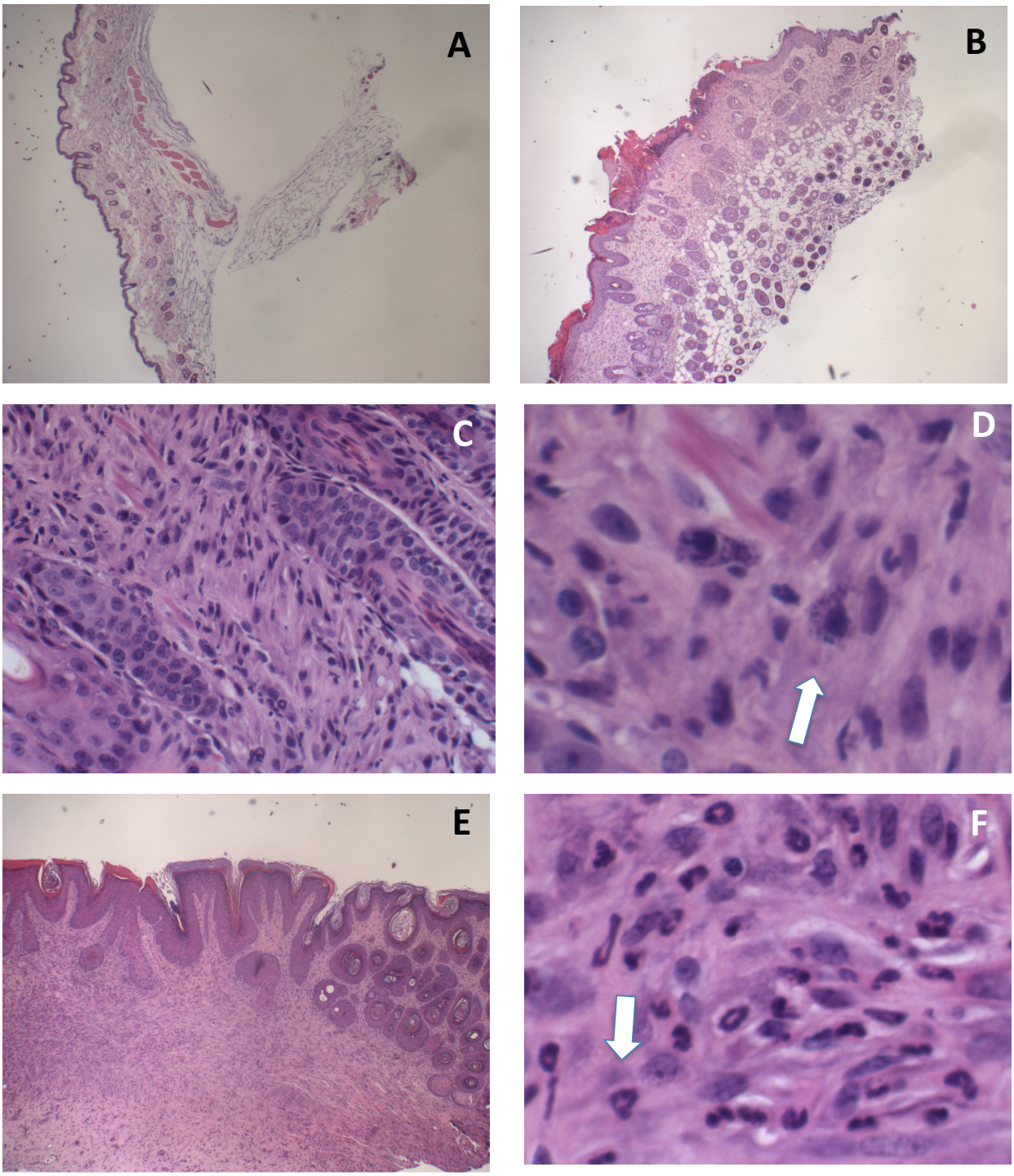

Figure 6.4 Dermatitic Il17d-/- skin harbors neutrophil and mast cells. (**A**) Control (contralateral) skin and (**B-D**) inflamed skin of *Il17d*-/- mice with dermatitis (626 days old). (**E, F**) Inflamed skin of *Il17d*-/- mice with dermatitis (597 days old). White arrow indicates presence of (**D**) mast cell and (**F**) neutrophil.

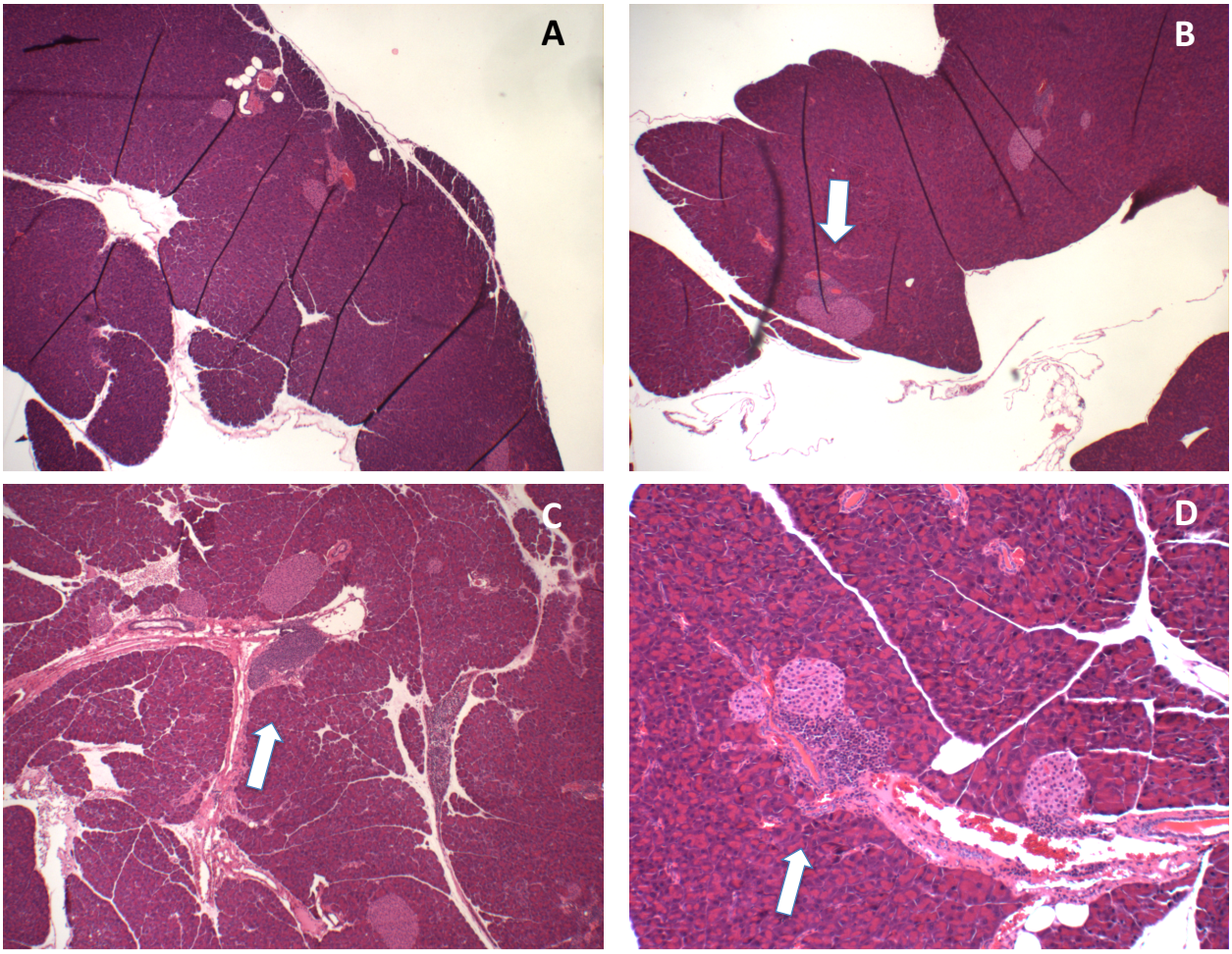

Figure 6.5 Il17d-/- pancreas have higher rates of islet inflammation. (**A**) Representative pancreas of aging wild-type C57BL/6 (WT 660 days old). (**B-D**) Representative images of *Il17d*-/- pancreas (569-641 days old) with islet inflammation. White arrows indicate immune cell infiltration. Images are 10x (A, B), 40x (C), and 100x (D) magnification.

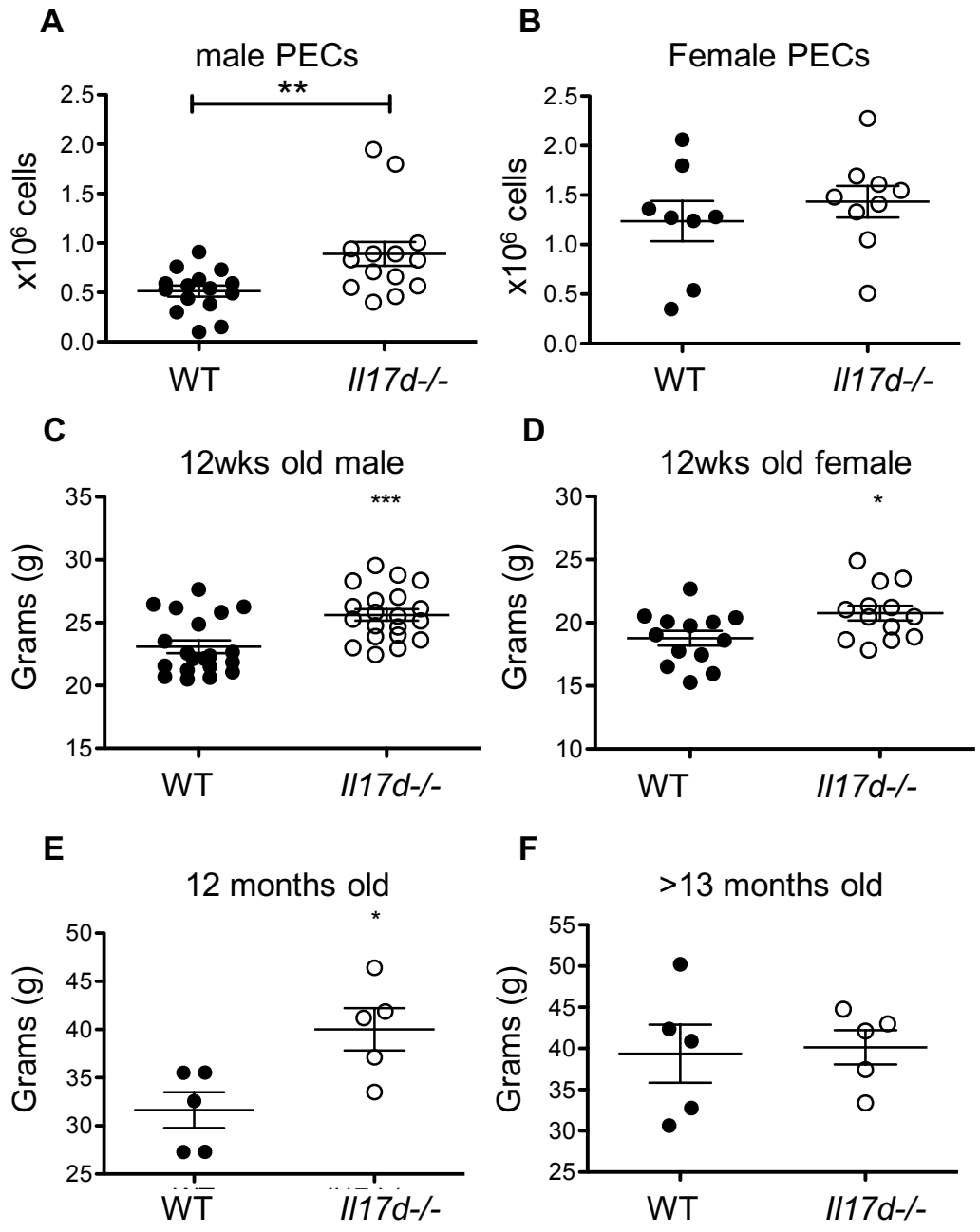

Figure 6.6 Higher weight and peritoneal cells in *Il17d*-/- mice. (**A**) Absolute number of peritoneal exudate cells in WT versus Il17d-/- male and (**B**) female mice. (**C**) Weight of WT versus Il17d-/- male and (**D**) female mice. (**E**) Weight of 12 months old and (**F**) more than 13 months old mice. Representative data from matched sex and age. *, $P < 0.05$; **, $P < 0.01$; ***, $P < 0.001$.

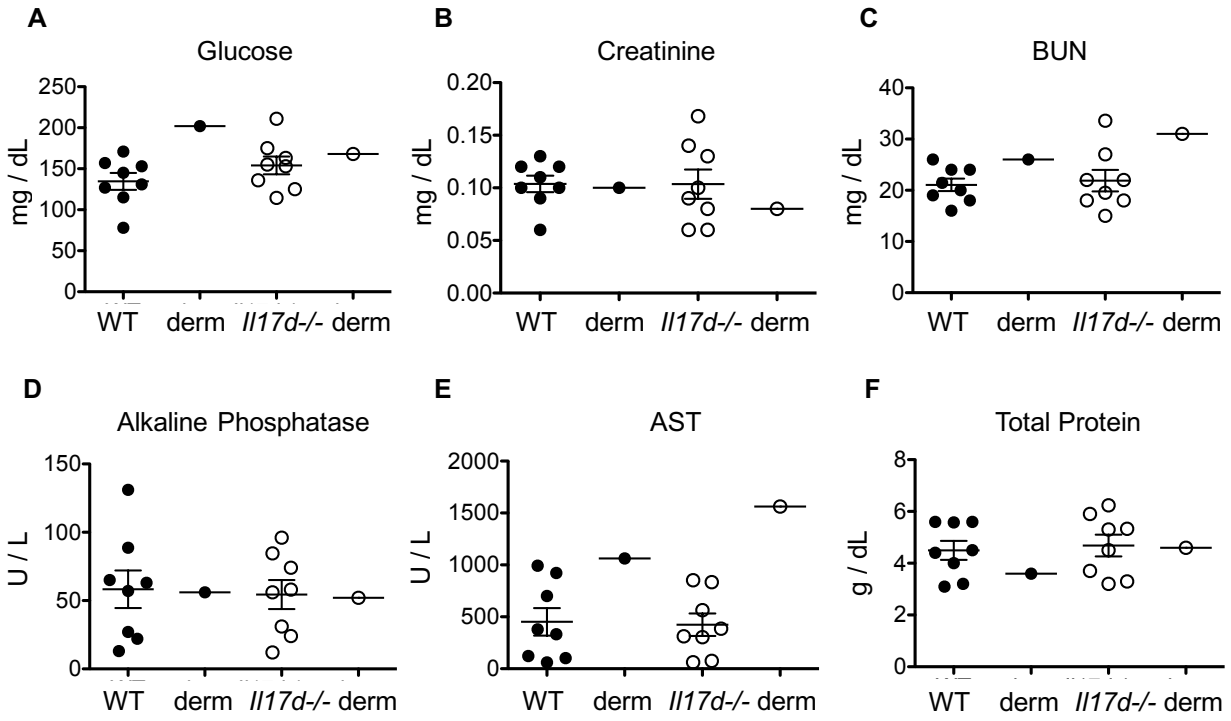

Figure 6.7 Metabolic values of *Il17d*-/- serum does not significantly differ from WT mice. Metabolic analyses were conducted on serum from 300-600 days old wild-type C57BL/6 wild-type (WT) and Il17d-/- mice with and without dermatitis for (**A**) glucose, (**B**) creatinine, (**C**) blood urea nitrogen (BUN), (**D**) alkaline phosphatase, (**E**) aspartate aminotransferase (AST), and (**F**) total protein. Data shown are mean ± SEM and are representative of 2 combined experiments.

CHAPTER VII: CONCLUSION

IL-17D is a gene that is expressed in vertebrates and invertebrates, and is one of the most ancient cytokines in its family (Chapter I). IL-17D is widely expressed in tissues such as brain, muscle, and kidney (16), and has been found to be positively regulated through infection by virus (8-10) and by living bacteria (Chapter V). Studies of regulatory elements surrounding IL-17D found that the anti-oxidant master regulator Nrf2 induces IL-17D (8); indeed, lower IL-17D transcript is found in bacteria-infected cells treated with ROS scavengers (Chapter V). Considering that bacterial infection by species such as Group A Streptococcus (GAS) generates reactive oxygen species (ROS) (45, 51), our data, combined with previous reports, point to a conserved defense mechanism of multicellular organisms that involve IL-17D in responses against harmful stressors.

At first glance, our data in Chapter II presents a nuanced property of IL-17D: different cell types respond differently. However, it is possible that IL-17D induces not only pro-inflammatory, but also potentially anti-inflammatory genes. In fact, there have been reports supporting the view on immune-suppressive effects of IL-17D. Initial reports by Starnes and colleagues had claimed IL-17D to inhibit proliferation of myeloid progenitors (16). Recent findings by Lee and colleagues demonstrate IL-17D to attenuate CD8 T cell activity in vivo (44). Indeed, the claim for a possible role of IL-17D in tissue homeostasis is warranted. As we have found in Chapter VI, *Il17d*-/- mice develop higher rate of dermatitis after the age of 1-year old, placing this cytokine in the physiology of healing processes and/or anti-inflammatory homeostasis instead of the much anticipated pro-inflammatory role.

The effect of IL-17D on non-immune cells has only been reported as pro-inflammatory (8-10, 16). However, we saw in Chapter II that IL-17D induces genes involved in melanogenesis,

such as *Dct*, *Pax3*, and *Sox10*. Although melanin production has long established its importance in the context of photoprotective and antioxidant processes in the skin, ties to immunoregulation are just emerging (21). Our results from Chpater II potentially offer an explanation for the dualilty of pro-inflammatory (6-10, 16, Chapter III-V) and anti-inflammatory (16, 44, Chapter VI) role IL-17D seem to have in regulating inflammation, especially in the context of responding to oxidative stress.

Melanogenesis genes are of particular interest due to known anti-inflammatory role of melanin. For example, from a pathogen perspective, organisms such as fungi have been characterized to produce melanin as a defense mechanism to quench the reactive oxygen species produced by hostile host (70). From a host perspective, melanin is also employed similarly to accomplish the anti-inflammatory effect. Most notably, Mimura and colleagues reported in 1987 the anti-inflammatory effects of squid melanin in rats harboring carrageenan-induced edema (71). More recently, Kunwar and colleagues have shown melanin to attenuate production of pro-inflammatory cytokines such as IL-6 and also reduce oxidative stress in hepatic cells (72).

These above reports on melanin are in line with our previous observation of Nrf2 (generally known as anti-inflammatory transcription factor) inducing IL-17D. Oxidative stress induces IL-17D, which could possibly have an impact on promoting melanin synthesis in the epidermis. Since melanocyte activity such as melanin production depends on surrounding cells such as keratinocytes, we speculate that IL-17D is one of many growth factors and cytokines secreted from keratinocytes that activate protective melanin synthesis.

This dissertation, however, focused mostly on the pro-inflammatory properties of IL-17D, which was explored in the context of bacterial infection. We demonstrated that *Il17d*-/- mice are more prone to increased death and weight loss upon opportunistic GAS infection,

although with modest effect. We did not see major differences in bacterial burden in organs such as the spleen and the lung. However, our data suggests IL-17D is expressed in the kidney and has protective effect in bacterial infection. We speculate that pro-inflammatory effects of IL-17D had minimal effect on the overall survival of infected mice due to the redundancy with other cytokines that induce overlapping downstream effectors, such as IL-17A (discussed in Chapter II).

We measured increase in *Il17d* and *Ccl2* upon *in vivo* GAS infection of the wild-type (WT) kidney. We also detected trend for lower neutrophil infiltration and relatively lower *Ccl2* transcript in the *Il17d*-/- kidney compared to WT (Chapter IV). Generally speaking, kidney has relatively low ratio of immune cells to non-immune cells, compared to organs such as lungs and spleen (Chapter III). As such, organs with relatively lower resident immune cells may depend more so on recruitment in the event of local infection. We showed that recombinant IL-17D induces Ccl2 in vivo and also recruit neutrophils into the instilled site. Taken together, our data suggests *Il17d*-/- mice have impairment in some chemokine production.

Since the kidney is relatively lower in resident immune cells compared to organs such as lung and spleen, we speculate that *Il17d*-/- mice may face greatest disadvantage in warding off bacterial infection in organs dependent on effective recruitment of active responders. In fact, viral infection in *Il17d*-/- mice had also found kidney with higher burden than WT (9). Impaired recruitment or perhaps activation at the infected sites thus translates into higher bacterial CFU we observed in organ homogenates. In sum, our data presented in Chapter III, IV, and V suggests a partial role for IL-17D in mammalian anti-bacterial immunity, whereby *Ccl2* is induced and neutrophil is recruited into lesions burdened with actively replicating bacteria.

Chapter VII, in part, is an adapted version of the material that has been prepared for publication. **Washington A Jr**, Shirane K, Chan A, Lee D, Sasaki H, Bui JD. Differential expression analysis downstream of IL-17D. The dissertation author was the primary author of all material.

Chapter VII, in part, is an adapted version of the material that has been prepared for publication. **Washington A Jr**, Varki N, Valderrama JA, Nizet V, Bui JD. IL-17D mediates anti-bacterial immunity in Group A Streptococcus infection. Manuscript in preparation. The dissertation author was the primary author of all material.

Chapter VII, in part, is an adapted version of the material that has been prepared for publication. **Washington AJr**, Seelige R, Wilbur R, Varki N, Bui JD. Spontaneous ulcerative dermatitis in aging IL-17D knockout mice. The dissertation author was the primary author of all material.

APPENDIX A: MATERIALS AND METHODS

Mice

The UCSD Institutional Animal Care and Use Committee approved all animal use and procedures (protocol #S06201). All mice were housed in specific pathogen-free conditions prior to use. C57BL/6 mice were injected intraperitoneally with 200μL phosphate buffered saline (PBS) containing indicated concentrations of Group A Streptococcus (GAS). The serotype M1 GAS and the M1 mutant GAS were gifted from V. Nizet. The inoculum was prepared by growing GAS overnight in Todd-Hewitt broth (Teknova) and adjusting the concentration according to the spectrophotometric O.D. 600 reading. Inoculum colony forming units (CFU) were confirmed by serial dilution plating on Todd-Hewitt agar (Teknova). For survival assessment, mice were monitored at least every 12 hours to record the body weight and survey the degree of lethargy.

In vitro GAS experiments

Wild-type GAS were grown overnight and the concentrations were determined by spectrophotometric O.D. 600 reading. Heat-killed GAS was prepared by placing at 65-75^{o}C for 5-10 minutes; absence of growth was confirmed by plating heat-killed GAS on Todd-Hewitt agar. The infection ratio of GAS:cultured cells were 1:1 unless specified. Cells were cultured in RPMI containing 2% FBS. The cell culture plates were spun at 1500 rpm for 5 minutes to facilitate contact between GAS and cultured cells. Cells were pre-treated for 1 hour with either N-Acetyl-L-cysteine (NAC) or ammonium pyrrolidinedithiocarbamate (PRDC) at a concentration of 0.6 μM and 0.4 μM respectively (Sigma). Final concentration of peptidoglycan was prepared as 1μg/mL (Invivogen).

Bacterial colony forming units assay

Peritoneal exudate and cells were collected by lavage with 2.5mL PBS. Biopsies of right kidney, spleen, right lung, liver, and the heart of each mouse was collected in order to determine GAS burden. The tissues were weighed and homogenized in 1mL PBS or RPMI medium containing 2% FBS through the 70μm strainer. Homogenized tissues were serially diluted 10-fold, and 50μL or 10μL from each aliquot were cultured overnight on Todd-Hewitt agar at 36.5^{o}C. The measurement of CFU/g was determined based on total CFU in 1mL divided by the weight of organ; samples without a colony were assigned as 1 CFU/mL and divided by the weight of the organ.

Antibodies and flow cytometry

Percentage leukocytes within each sample was determined using the flow cytometer. Following markers were employed to identify: B cells (CD45, B220), CD4 T cells (CD45, CD3, CD4), CD8 T cells (CD45, CD3, CD8), dendritic cells (CD45, MHCII, CD11c), monocytes (CD45, CD11b), macrophage (CD45, F4/80, MHCII), neutrophils (CD45, Ly6g), basophils/mast cells (CD45, FcERIa), eosinophils (CD45, F4/80, CD11b), non-immune cells (CD45 negative). All antibodies were purchased from Biolegend. 7AAD (Calbiochem) -positive cells were excluded as dead cells.

Quantitative real-time PCR

RNA was extracted using TRI-zol (Life Technologies) or by using the Direct-zol RNA MiniPrep Kit (Zymogen). cDNA was synthesized using the High-Capacity cDNA Reverse Transcription Kit (Applied Biosystems); qPCR data were generated using SYBR Green mix

(Applied Biosystems) with forward and reverse primers of indicated genes; reaction was run on the One Step Plus Real-Time PCR System (all from Applied Biosystems). Samples were normalized based on expression of *Hprt* or *Gapdh* reference gene. Relative gene expression was determined based on three biological replicates and figures show one representative experiment. The primer sequences are listed in the Table.

Histology

Organs were fixed overnight at 25°C in 10% neutral buffered formalin, embedded in paraffin, sectioned and stained with hematoxylin and eosin by the UCSD Histology Core. Neutrophils were stained for by monoclonal anti-myeloperoxidase antibody. Images were acquired on a Nikon Eclipse TE300 microscope.

RNA Sequencing

Total RNA from SVEC and B16 cell lines were extracted using TRIzol reagent (Life Technologies) according to the manufacterer's protocol. cDNA libraries were prepared using TruSeq non-Stranded Total RNA Sample Prep Kit (Illumina) according to manufacturer's instructions. cDNA libraries were sequenced with a HiSeq2500 (Illumina). Data was processed through DESeq2 (74).

Microarray

Cells in culture were incubated with siRNA for 18 hours prior to analysis. Total RNA from B16 cell lines were extracted using PureLink RNA Mini Kit (Invitrogen) according to the manufacterer's protocol. cRNA synthesis was conducted using TotalPrep RNA Amplification

Kit (Invitrogen). cRNA was hybridized using MouseWG-6 v2.0 Expression BeadChip (Illumina). Data was analyzed and heatmap created through GenePattern (Broad Institute).

Cytokine injection

C57BL/6 mice were maintained under specific pathogen-free conditions. 0.5μg of IL-17D (R&D) in 250μL PBS or vehicle in PBS were i.p. injected per mouse. After 4hours, mice were euthanized using carbon dioxide, and peritoneal cavity was lavaged in total 10mL PBS containing 1% FBS. Cells were incubated in RBC lysis buffer (Biolegend) and counted using the hemocytometer.

Peripheral blood analysis

Circulating blood from 300-600 days old mice was obtained via submandibular puncture with 4mm or 5mm sterile animal lancet (MEDIpoint). For complete blood count and RBC measurements, tubes with EDTA were used to collect the blood, and analyzed using Hemavet (Drew Scientific) at the UCSD Hematology Core. For metabolic panel analysis, serum was obtained by leaving the blood in room temperature for 30 minutes and centrifuging at 13,000 rpm for 10 minutes. Serum was analyzed by the UCSD Center for Advanced Laboratory Medicine.

Statistical analysis

All statistical analyses were processed through a statistical software package (GraphPad Prism). Kaplan-Meier survival curves were generated and analyzed using the log-rank test in order to assess statistical significance. CFU data from organ homogenates and lavage were

analyzed using the nonparametric Mann-Whitney *U* test. In vitro GAS incubation experiments were analyzed using the Student's two-tailed t-test. All P-values less than 0.05 were considered to be significant. P values are denoted in figures as; * $P<0.05$, ** $P<0.01$, *** $P<0.005$.

APPENDIX B: SUPPLEMENTAL TABLE I

SVEC+IL17A	**adj pvalue**	**SVEC+IL17D**	**adj pvalue**
Ccl2	1.11E-12	**Cebpd**	3.43E-12
Ccl7	1.11E-12	**Erdr1**	1.20E-11
Zc3h12a	1.11E-12	Hspa1a	9.38E-10
Cxcl1	4.30E-09	Rn45s	9.86E-10
Cebpd	9.17E-09	Ccdc85b	1.26E-08
Igf2	1.09E-08	Gpnmb	1.49E-06
Steap4	5.53E-08	**H2afj**	7.27E-06
Vnn1	0.00010	Rnaseh2c	1.94E-05
Lrig1	0.00012	**Ccl2**	2.61E-05
Cxcl5	0.00027	Zfp580	2.77E-05
Mest	0.00027	Slc25a29	3.49E-05
Myc	0.00032	**Ier3**	6.43E-05
Itpk1	0.00032	Scand1	7.31E-05
Nfkbiz	0.00033	Hotairm1	7.31E-05
Gpc3	0.00074	Pax3	7.31E-05
Ntn1	0.00074	Nes	7.31E-05
Fas	0.00193	Map1s	7.36E-05
Meg3	0.00193	Hist1h1c	9.29E-05
Cdkn1c	0.00193	Slc2a6	0.00018
A930015D03Rik	0.00208	Crlf2	0.00019
Slc11a2	0.00208	**Zc3h12a**	0.00019
Nos2	0.00265	Col6a4	0.00019
Spp1	0.00296	Ctu1	0.00025
Cxcl16	0.00341	Jund	0.00025
Igfbp5	0.00368	Hist1h2ag	0.00025
Casp4	0.00378	Gm10825	0.00086
Mrvi1	0.00637	Kank4	0.00090
Nfkbia	0.00838	Zfp787	0.00092
Ifnar2	0.01042	Ier5l	0.00092
Hmga1	0.01044	2810428I15Rik	0.00150
Relb	0.01059	Mlph	0.00167
Bcl3	0.01166	Hspa1b	0.00171
Erdr1	0.01166	Plekhg6	0.00171
Ier3	0.01166	Tspan10	0.00171
Rhbdf2	0.01166	Arfgef3	0.00180

Stx6	0.01166	2310036O22Rik	0.00234
Atg9b	0.01812	Rhbdl1	0.00234
Pik3r5	0.02524	Prickle1	0.00234
Ptprb	0.02524	Zbed5	0.00241
Egr2	0.02559	Scarf2	0.00348
Foxs1	0.02562	**Chst7**	0.00401
Adam12	0.02796	Zfp575	0.00452
Mdk	0.02796	Hnrnpa0	0.00520
Ovgp1	0.02796	6030419C18Rik	0.00620
H2afj	0.02844	Twist2	0.00620
Saa3	0.03886	Bola1	0.00620
Chst7	0.04392	Apoe	0.00620
Tgfbi	0.04392	Myo7a	0.00620
Osbpl3	0.04556	2310009B15Rik	0.00760
Tmem176b	0.04947	Clvs1	0.00760
		Rabac1	0.00784
		Cited2	0.00857
		Crebzf	0.00857
		Slc24a5	0.00857
		Eid2b	0.00880
		Zfp771	0.00889
		Slc36a2	0.00913
		Mgat4b	0.00916
		Slc6a17	0.00976
		Mlana	0.00987
		Ccdc40	0.01024
		Prickle4	0.01099
		Acbd6	0.01168
		Nfkbiz	0.01168
		Rrad	0.01168
		Parvb	0.01168
		Fosl1	0.01476
		Zfpm1	0.01531
		Gcnt3	0.01556
		Sap30	0.01592
		Limch1	0.01655
		Fuz	0.01861
		Fkbp6	0.01861
		Tyr	0.01902

		Zfp622	0.01929
		Syt4	0.01929
		Nptxr	0.01968
		Zfp865	0.02031
		Cxcl1	0.02148
		Tfap2a	0.02215
		Exd1	0.02330
		Rpl36	0.02346
		Mrpl52	0.02350
		Rplp2	0.02416
		Fbxl16	0.02416
		Nrcam	0.02543
		Igfbp6	0.02675
		Zfyve21	0.02748
		Gabre	0.02771
		Mypop	0.02771
		Rpl27a	0.02784
		Cahm	0.02784
		Abca12	0.02798
		Fxyd5	0.02873
		Zfp628	0.02895
		Serf1	0.02986
		Pgls	0.03044
		Cebpb	0.03153
		Hist1h2be	0.03390
		Zscan4b	0.03390
		Icam4	0.03390
		Hmga1	0.03400
		Plcxd2	0.03400
		Isl2	0.03400
		Mir3101	0.03478
		Eva1b	0.03508
		Sox11	0.03628
		Hoxd9	0.03781
		Ppp1r35	0.03786
		Sap30l	0.03841
		Taf4b	0.03841
		Zfp385c	0.03925
		Mrpl34	0.04004

		Car6	0.04059
		Prkcq	0.04238
		F8a	0.04289
		Junb	0.04304
		Ubap1l	0.04396
		Zfp768	0.04407
		Ndufc1	0.04505
		Btbd19	0.04648
		A330035P11Rik	0.04662
		Numbl	0.04703
		Itpk1	0.04733
		Tmc8	0.04767
		Snora65	0.04969

APPENDIX C: SUPPLEMENTAL TABLE II

B16 + IL-17D	Positive Log2 FC	**B16 + IL-17D**	Negative Log2 FC
Slc7a11	0.313	Rps29	-0.458
Taf9b	0.212	Rplp2	-0.339
L1cam	0.211	Rplp1	-0.314
Lgals9	0.192	Rpl36	-0.310
Nfat5	0.187	Rps28	-0.290
Cdip1	0.183	Rps20	-0.279
Lipa	0.181	Cox5a	-0.272
Sec24d	0.180	Rpl27a	-0.266
Gstm1	0.180	Rpl39	-0.260
Sec24b	0.178	Rpl32	-0.260
Nfatc1	0.176	Shfm1	-0.259
Lpp	0.175	Rps27a	-0.259
Myadm	0.174	Rpl36al	-0.257
Tecr	0.174	Mrps24	-0.256
Shisa5	0.173	Tomm7	-0.253
Gm6682	0.171	Atp5k	-0.247
Nif3l1	0.168	Hint1	-0.240
Slc4a4	0.168	Rpl8	-0.237
Gclc	0.168	Hnrnpa0	-0.236
Zscan22	0.167	Mrto4	-0.233
Hipk2	0.167	Exosc6	-0.232
Vgll3	0.167	Lsm5	-0.230
AW549877	0.167	Uqcrh	-0.229
Atn1	0.166	2310036O22Rik	-0.229
Dhcr7	0.165	Rps19	-0.228
Wnk1	0.164	Rps9	-0.227
Dagla	0.163	Rpl9	-0.226
Polr2a	0.163	Rpl13	-0.226
Cxcl10	0.163	Hmgn1	-0.224
Proser1	0.162	Sf3b5	-0.223
Pcolce	0.162	Rps16	-0.222
Scmh1	0.162	Tpt1	-0.222
Grina	0.160	Rnaseh2c	-0.221
Arsb	0.160	Rpl23	-0.216
Syngr2	0.159	Mrpl52	-0.214

Sf3b4	0.158	Spr	-0.213
Srcap	0.156	Rps17	-0.212
Wisp1	0.156	Ndufab1	-0.211
Rnasek	0.156	Timm13	-0.211
Akna	0.155	Zbed5	-0.210
Zmiz1	0.155	Rps15a	-0.206
Rad9a	0.155	Rpl22	-0.205
Ints9	0.154	Apoe	-0.203
Ero1l	0.153	Rpl34	-0.203
Gpr137b-ps	0.152	Polr2f	-0.202
Wbp2	0.152	Ndufa1	-0.202
Atp6v0a1	0.152	Cox17	-0.201
Synj1	0.151	Rpl37a	-0.200
G6pdx	0.150	Crocc	-0.199
Rnf38	0.150	Mphosph6	-0.199
Atf7	0.149	Tmem242	-0.198
Wasf2	0.148	Abhd17a	-0.198
Tead1	0.146	Ostf1	-0.196
Ankhd1	0.146	Hspa5	-0.195
Ost4	0.145	Oaz1	-0.195
Raph1	0.145	Mafg	-0.195
Pom121	0.144	Metrn	-0.192
Ube2m	0.144	Mrfap1	-0.192
Tns2	0.144	Edf1	-0.191
Rere	0.143	Rps8	-0.188
Arhgef11	0.141	Polr1d	-0.188
Ago2	0.140	Yeats4	-0.187
Arid1a	0.139	Eif1ax	-0.187
Fn1	0.139	Bloc1s1	-0.187
Grn	0.138	Cadm4	-0.187
Capns1	0.137	Tmem160	-0.184
Wdyhv1	0.136	Pfdn1	-0.183
Lamp2	0.135	Galk1	-0.182
Dot1l	0.135	Higd1a	-0.181
Pprc1	0.132	Ndufb7	-0.180
Arhgap21	0.132	Rps27	-0.180
Tpp1	0.130	Nol7	-0.178
Cic	0.129	Rpl17	-0.178
Tex2	0.128	Rpl13a	-0.178

Cryab	0.126	Snhg6	-0.177
Tuba1c	0.121	Myl6	-0.177
Lasp1	0.121	Hnrnpa2b1	-0.174
Laptm4a	0.120	Ndufb11	-0.172
Srrm2	0.116	Rpa3	-0.172
Tuba1a	0.116	Nr2f6	-0.171
Slc6a6	0.115	Atp5l	-0.171
Podxl	0.113	Nme1	-0.171
Lhx9	0.069	Lsm8	-0.170
Nr5a1	0.068	Ccdc85b	-0.169
Gata4	0.054	Dmrta2	-0.167
Emx2	0.049	Sub1	-0.167
AW551984	0.044	Hmg20b	-0.167
		Sec61g	-0.166
		Nom1	-0.166
		Rpl23a	-0.166
		Creld2	-0.165
		Exosc3	-0.165
		Ndufa7	-0.164
		Gm5643	-0.164
		Rpl11	-0.164
		Ddx23	-0.163
		Naca	-0.163
		Rpl36a	-0.163
		Ndufb9	-0.163
		Rps15	-0.162
		Hspd1	-0.161
		Zcrb1	-0.161
		Ndufb6	-0.160
		Atp5a1	-0.160
		Tbca	-0.160
		Fam50a	-0.159
		Ccdc12	-0.158
		Snrnp70	-0.158
		Fkbp3	-0.158
		Gm9833	-0.158
		Rrp15	-0.157
		Itga9	-0.157
		Lzts2	-0.157

		Tmem256	-0.157
		Tmf1	-0.156
		Nme2	-0.156
		Psmc2	-0.156
		2310047M10Rik	-0.156
		Rpl28	-0.155
		Rps15a-ps6	-0.154
		Lamtor4	-0.154
		Tipin	-0.153
		Gripap1	-0.153
		Ppp1r14b	-0.153
		Magohb	-0.153
		Rdh14	-0.152
		Maz	-0.152
		Cct2	-0.151
		Dbi	-0.150
		Rnf10	-0.150
		Mgat4b	-0.150
		Arpc1b	-0.150
		Eif3b	-0.150
		Rpl21	-0.149
		Rrp1	-0.149
		Atp5j	-0.148
		Bax	-0.148
		Cox8a	-0.148
		Rps13	-0.147
		Hnrnpul2	-0.147
		Gm6654	-0.147
		Rpl14	-0.147
		Mpc2	-0.146
		Rpl22l1	-0.146
		Grcc10	-0.146
		Anp32e	-0.145
		Rpl18	-0.144
		Uqcrq	-0.143
		Hnrnpm	-0.143
		Atp13a2	-0.142
		Drap1	-0.142
		Dnajc7	-0.141

		Nudt3	-0.140
		Rps24	-0.140
		Uba52	-0.140
		Hnrnpab	-0.139
		Cox6b1	-0.138
		Eef1g	-0.138
		Sdhb	-0.137
		Rangap1	-0.135
		Cbx3	-0.135
		Lmna	-0.134
		Fabp5	-0.131
		Dnaja1	-0.131
		Eif1	-0.128
		Cox5b	-0.128
		Eif5b	-0.128
		Psmd7	-0.125
		Rps4x	-0.125
		Rpl6	-0.124
		Aldh2	-0.123
		Rps7	-0.120

APPENDIX D: SUPPLEMENTAL TABLE III

B16 + **IL17A**	Log2FC	B16 + **IL17D**	Log2FC
Slc7a11	0.378	**Slc7a11**	0.313
Zc3h12a	0.329	Taf9b	0.212
Nfkbiz	0.306	**L1cam**	0.211
Ier3	0.28	Lgals9	0.192
Malat1	0.269	Nfat5	0.187
Tubb3	0.261	Cdip1	0.183
C77080	0.235	Lipa	0.181
Trp53	0.214	Gstm1	0.18
Mcam	0.208	Sec24b	0.178
Hspg2	0.203	Myadm	0.174
Csf1	0.198	Tecr	0.174
Lpp	0.198	Gm6682	0.171
Slc11a2	0.195	Hipk2	0.167
Tapbp	0.193	Vgll3	0.167
Cdkn1a	0.191	Atn1	0.166
Kmt2d	0.189	Dhcr7	0.165
Wdyhv1	0.182	Wnk1	0.164
Parp3	0.181	Dagla	0.163
Tnrc6b	0.175	Polr2a	0.163
Nfkb2	0.167	**Cxcl10**	0.163
Leng8	0.166	Pcolce	0.162
Fgfr1op	0.163	Syngr2	0.159
Rc3h1	0.16	Sf3b4	0.158
Adamts1	0.159	Srcap	0.156
L1cam	0.157	Wbp2	0.152
Cxcl10	0.156	Atp6v0a1	0.152
Mbd6	0.156	G6pdx	0.15
Tgfb1	0.155	Podxl	0.113
Ecscr	0.15	Lhx9	0.069
Cpsf6	0.149	Nr5a1	0.068
Anxa1	0.147	Emx2	0.049
Rgs16	0.146		
Laptm4a	0.142		
Actg1	0.137		

Relb	0.121		
Map3k8	0.085		
Cxcl1	0.07		

REFERENCES

1. Pappu R, Rutz S, and Ouyang W. Regulation of epithelial immunity by IL-17 family cytokines. *Trends Immunol*. 2012;33:343-349.

2. Kono T., H. Korenaga, and M. Sakai. Genomics of fish IL-17 ligand and receptors: A review. *Fish Shellfish Immunol*. 2011;31:635-643.

3. Hibino T, Loza-Coll M, Messier C, Majeske AJ, Cohen AH, Terwilliger DP, Buckley KM, Brockton V, Nair SV, Berney K, Fugmann SD, Anderson MK, Paner Z, Cameron RA, Smith LC, and Rast JP. The immune gene repertoire encoded in the purple sea urchin genome. *Dev Biol.* 2006;300:349–65.

4. Roberts S, Gueguen Y, de Lorgeril J, and Goetz F. Rapid accumulation of an interleukin 17 homolog transcript in Crassostrea gigas hemocytes following bacterial exposure. *Dev. Comp. Immunol*. 2008;32(9):1099-104.

5. He Y, Jouaux A, Ford SE, Lelong C, Sourdaine P, Mathieu M, and Guo X. Transcriptome analysis reveals strong and complex antiviral responses in a mollusc. Fish Shellfish Immunol. 2015;46:131-44.

6. O'Sullivan TE, Saddawi-Konefka R, Gross E, Tran M, Mayfield SP, Ikeda H, and Bui JD. Interleukin-17D mediates tumor rejection through recruitment of natural killer cells. *Cell Report*. 2014;7:989–998.

7. Saddawi-Konefka R, O'Sullivan TE, Gross ET, Washington A Jr, and Bui JD. Tumor-expressed IL-17D recruits NK cells to reject tumors. *Oncoimmunol.* 2015;3(12): e954853.

8. Saddawi-Konefka R, Seelige R, Gross ET, Levy E, Searles SC, Washington A Jr, Santosa EK, Liu B, O'Sullivan TE, Harismendy O, and Bui JD. Nrf2 Induces IL-17D to Mediate Tumor and Virus Surveillance. *Cell Report*. 2016;16:2348-58.

9. Seelige R, Saddawi-Konefka R, Adams NM, Picarda G, Sun JC, Benedict CA, and Bui JD. Interleukin-17D and Nrf2 mediate initial innate immune cell recruitment and restrict MCMV infection. *Sci. Reports.* 2018;8(1):13670.

10. Seelige R, Washington A Jr, and Bui JD. The ancient cytokine IL-17D is regulated by Nrf2 and mediates tumor and virus surveillance. *Cytokine*. 2016;91:10-12.

11. O'Sullivan T, Saddawi-Konefka R, Vermi W, Koebel CM, Arthur C, White JM, Uppaluri R, Andrews DM, Ngiow SF, Teng MW, Smyth MJ, Schreiber RD, and Bui JD. Cancer immunoediting by the innate immune system in the absence of adaptive immunity. *J Exp Med*. 2012;209:1869–82.

12. Shankaran V, Ikeda H, Bruce AT, White JM, Swanson PE, Old LJ, and Schreiber RD. IFNgamma and lymphocytes prevent primary tumour development and shape tumour immunogenicity. *Nature*. 2001;410:1107–11.

13. Korn T, Bettelli E, Oukka M, and Kuchroo VK. IL-17 and Th17 cells. *Ann Rev Immunol*. 2009;27:485-517.

14. Kolls JK, and Linden A. Interleukin-17 family members and inflammation. *Immunity*. 2004;21(4):467-476.

15. McGeachy MJ, Cua DJ, and Gaffen SL. The IL-17 family of cytokines in health and disease. *Immunity*. 2019;50(4): 892-906.

16. Starnes T, Broxmeyer HE, Robertson MJ, and Hromas R. Cutting Edge: IL-17D, a novel member of the IL-17 family, stimulates cytokine production and inhibits hemopoiesis. *J Immunol*. 2002;169: 642-646.

17. Dufour JH, Dziejman M, Liu MT, Leung JH, Lane TE, and Luster AD. IFN-g-inducible protein 10 (IP-10; CXCL10)-deficient mice reveal a role for IP-10 in effector T cell generartion and trafficking. *J Immunol*. 2002;168: 3195-3204.

18. Lu L, Pan K, Zheng HX, Li JJ, Qiu HJ, Zhao JJ, Weng DS, Pan QZ, Wang DD, Jiang SS, Chang AE, Li Q, and Xia JC. IL-17A promotes immune cell recruitment in human esophageal cancers and the infiltrating dendritic cells represent a positive prognostic marker for patient survival. *J immunother*. 2013;36(8): 451–8.

19. Cichorek M, Wachulska M, Stasiewicz A, and Tyminska A. Skin melanocytes: biology and development. *Postepy Dermatol Alergol*. 2013; 30(1): 30-41.

20. D'Mello SAN, Finlay GJ, Baguley BC, and Askarian-Amiri ME. Signaling pathways in melanogenesis. *Int J Mol Sci*. 2016;17(7): 1144.

21. ElObeid AS, Kamal-Eldin A, Abdelhalim MAK, and Haseeb AM. Pharmacological properties of malanin and its function in health. *Basic Clin Pharmacol Tosicol*. 2017;120(6):512-522.

22. Ma Q, Battelli L, Hubbs AF. Multiorgan autoimmune inflammation, enhanced lymphoproliferation, and impaired homeostasis of reactive oxygen species in mice lacking the antioxidant-activated transcription factor Nrf2. *Am J Pathol*. 2006; 168:1960–74.

23. Ma Q. Role of Nrf2 in oxidative stress and toxicity. *Annu Rev Pharmacol Toxcol*. 2013; 53:401-426.

24. Ramirez-Carrozzi V, Sambandam A, Luis E, Lin Z, Jeet S, Lesch J, Hackney J, Kim J, Zhou M, Lai J, Modrusan Z, Sai T, Lee W, Xu M, Caplazi P, Diehl L, de Voss J, Caalzs

M, Gonzalez L Jr, Singh H, Ouyang W, Pappu R. IL-17C regulates the innate immune function of epithelial cells in an autocrine manner. *Nat Immunol*. 2011;12: 1159–1166.

25. Yamaguchi Y, Fujio K, Shoda H, Okamoto A, Tsuno NH, Takahashi K, Yamamoto K. IL-17B and IL-17C are associated with TNF-alpha production and contribute to the exacerbation of inflammatory arthritis. *J Immunol*. 2007;179: 7128–7136.

26. Pappu R, Ramirez-Carrozzi V, and Sambandam A. The interleukin-17 cytokine family: critical players in host defence and inflammatory diseases. *Immunology*. 2011;134(1): 8–16.

27. Aujla SJ, Chan YR, Zheng M, Fei M, Askew DJ, Pociask DA, Reinhart TA, McAllister F, Edeal J, Gaus K, Husain S, Kreindler JL, Dubin PJ, Pilewski JM, Myerburg MM, Mason CA, Iwakura Y, Kolls JK. IL-22 mediates mucosal host defense against Gram-negative bacterial pneumonia. *Nat Med*. 2008;14(3): 275-81.

28. Hamada S, Umemura M, Shiono T, Tanaka K, Yahagi A, Begum MD, Oshiro K, Okamoto Y, Watanabe H, Kawakami K, Roark C, Born WK, O'Brien R, Ikuta K, Ishikawa H, Nakae S, Iwakura Y, Ohta T, and Matsuzaki G. IL-17A produced by gammadelta T cells plays a critical role in innate immunity against listeria monocytogenes infection in the liver. *J Immunol*. 2008;181(5): 3456-63.

29. Shibata K, Yamada H, Hara H, Kishihara K, and Yoshikai Y. Resident Vdelta1+ gammadelta T cells control early infiltration of neutrophils after Escherichia coli infection via IL-17 production. *J Immunol*. 2007;178(7): 4466-72.

30. Song X, Zhu S, Shi P, Liu Y, Shi Y, Levin SD, Qian Y. IL-17RE is the functional receptor for IL-17C and mediates mucosal immunity to infection with intestinal pathogens. *Nat Immunol*. 2011;12(12): 1151–8.

31. Ishigame H, Kakuta S, Nagai T, Kadoki M, Nambu A, Komiyama Y, Fujikado N, Tanahashi Y, Akitsu A, Kotaki H, Sudo K, Nakae S, Sasakawa C, Iwakura Y. Differential roles of interleukin-17A and -17F in host defense against mucoepithelial bacterial infection and allergic responses. *Immunity*. 2009;30(1): 108-19.

32. Fallon PG, Ballantyne SJ, Mangan NE, Barlow JL, Dasvarma A, Hewett DR, McIlgorm A, Jolin HE, McKenzie AN. Identification of an interleukin (IL)-25-dependent cell population that provides IL-4, IL-5, and IL-13 at the onset of helminth expulsion. *J Exp Med*. 2006;203: 1105–16.

33. Reynolds JM, Lee YH, Shi Y, Wang X, Angkasekwinai P, Nallaparaju KC, Flaherty S, Chang SH, Watarai H, and Dong C. Interleukin-17B Antagonizes Interleukin-25-Mediated Mucosal Inflammation. *Immunity*. 2015;42:692-703.

34. Kumari J, Larsen AN, Bogwald J, and Dalmo RA. Interleukin-17D in Atlantic salmon (Salmo salar): Molecular charaterization, 3D modeling and promoter analysis. *Fish Shellfish Immunol*. 2009;27: 647-659.

35. Tsutsui S, Nakamura O, and Watanabe T. Lamprey (Lethenteron japonicum) IL-17 upregulated by LPS-stimulation in the skin cells. *Immuonogenetics*. 2007;59: 873-882.

36. Zhang Q-L, Zhu Q-H, Liang M-Z, Wang F, Guo J, Deng X-Y, Chen J-Y, Wang Y-J, and Lin L-B. Comparative transcriptomic analysis provides insights into antibacterial mechanisms of Branchiostoma belcheri under Vibrio parahaemolyticus infection. *Fish Shellfish Immunol*. 2018;76: 196-205.

37. Moreira R, Milan M, Balseiro P, Romero A, Babbucci M, Figueras A, Bargelloni L, and Novoa B. Gene expression profile analysis of Manila clam (Ruditapes philippinarum) hemocytes after a Vibrio alginolyticus challenge using an immune-enriched oligo-microarray. *BMC Genomics*. 2014;15:267.

38. Buckley KM, Ho ECH, Hibino T, Schrankel CS, Schuh NW, Wang G, and Rast JP. IL17 factors are early regulators in the gut epithelium during inflammatory response to Vibrio in the sea urchin larva. *eLife*. 2017;6:e23481.

39. Huang J, Meng S, Hong S, Lin X, Jin W, and Dong C. IL-17C is required for lethal inflammation during systemic fungal infection. *Cell Mol Immunol*. 2016;13:474-483.

40. Conti HR, Whibley N, Coleman BM, Garg AV, Jaycox JR, and Gaffen SL. Signaling through IL-17C/IL-17RE is dispensable for immunity to systemic, oral and cutaneous candidiasis. *PLoS One*. 2015;10(4):e0122807.

41. Li L, Huang L, Vergis AL, Ye H, Bajwa A, Narayan V, Strieter RM, Rosin DL, Okusa MD. IL-17 produced by neutrophils regulates IFN-g-mediated neutrophil migration in mouse kidney ischemia-repersion injury. *J Clin Invest*. 2009;120:331-342.

42. Yamaguchi S, Nambu A, Numata T, Yoshizaki T, Narushima S, Shimura E, Hiraishi Y, Arae K, Morita H, Matsumoto K, Hisatome I, Sudo K, and Nakae S. 2018. The roles of IL-17C in T cell-dependent and –independent inflammatory diseases. *Sci Reports*. 2018;8:15750.

43. Haque A, Kajiwara C, Matsumoto T, Ishii Y, and Tateda K. IL-17A/IL-17F double KO mice are resistant to lipopolysaccharide induced endotoxic shock. *Eur Exp Biol*. 2017;7:14.

44. Lee Y, Clinton J, Yao C, and Chang SH. Interleukin-17D promotes pathogenicity during infection by suppressing CD8 T cell activity. *Front Immunol*. 2019; 10:1172.

45. Fieber C, and Kovarik P. Responses of innate immune cells to group A Streptococcus. Front. *Cell Infect Microbiol*. 2014;4: 1-7.

46. Matzinger P. The danger model: a renewed sense of self. *Science*. 2002; 296:301-305.

47. Vance RE, Isberg RR, and Portnoy DA. Patterns of pathogenesis: discrimination of pathogenic and nonpathogenic microbes by the innate immune system. *Cell Host & Microbe*. 2009;6(1): 10–21.

48. Sander LE, Davis MJ, Boekschoten MV, Amsen D, Dascher CC, Ryffel B, Swanson JA, Muller M, and Blander JM. Detection of prokaryotic mRNA signifies microbial viability and promotes immunity. *Nature*. 2011;474:385-389.

49. Moretti J, Roy S, Bozec D, Martinez J, Chapman JR, Ueberheide B, Lamming DW, Chen ZJ, Horng T, Yeretssian G, Green DR, and Blander JM. STING senses microbial viability to orchestrate stress-mediated autophagy of the endoplasmic reticulum. *Cell*. 2017;171:809-823.

50. Aikawa C, Nozawa T, Maruyama F, Tsumoto K, Hamada S, Nakagawa I. Reactive oxygen species induced by Streptococcus pyogenes invasion trigger apoptotic cell death in infected epithelial cells. *Cell Microbiol*. 2010;12(6): 814-30.

51. Regnier E, Grange PA, Ollagnier G, Crickx E, Elie L, Chouzenoux S, Weill B, Plainvert C, Poyart C, Batteux F, and Dupin N. Superoxide anions produced by Streptococcus pyogenes group A-stimulated keratinocytes are responsible for cellular necrosis and bacterial growth inhibition. *Innate Immunity*. 2016;22(2): 113–123.

52. Boncompain G, Schneider B, Delevoye C, Kellermann O, Dautry-Varsat A, and Subtil A. Production of Reactive Oxygen Species Is Turned On and Rapidly Shut Down in Epithelial Cells Infected with Chlamydia trachomatis. *Infect Immun*. 2010;78(1): 80-87.

53. Rouvier E, Luciani MF, Mattei MG, Denizot F, and Golstein P. CTLA-8, cloned from an activated T cell, bearing AU-rich messenger RNA instability sequences, and homologous to a herpesvirus saimiri gene. *J Immunol*. 1993;150:5445–56.

54. Ivanov II, McKenzie BS, Zhou L, Tadokoro CE, Lepelley A, Lafaille JJ, Cua DJ, Littman DR. The orphan nuclear receptor RORgammat directs the differentiation program of proinflammatory IL-17(+) T helper cells. *Cell*. 2006;126:1121-1133.

55. Yang XO, Pappu BP, Nurieva R, Akimzhanov A, Kang HS, Chung Y, Ma L, Shah B, Panopoulos AD, Schluns KS, Watowich SS, Tian Q, Jetten AM, Dong C. T helper 17 lineage differentiation is programmed by orphan nuclear receptors ROR alpha and RORgamma. *Immunity*. 2008;28:29–39.

56. Pfeifer P, Voss M, Wonnenberg B, Hellberg J, Seiler F, Lepper PM, Bischoff M, Langer F, Schäfers HJ, Menger MD, Bals R, and Beisswenger C. IL-17C is a mediator of respiratory epithelial innate immune response. *Am J Respir Cell Mol Biol*. 2013;48:415–421.

57. von Moltke J, Ji M, Liang H-E, and Locksley RM. Tuft-cell-derived IL-25 regulates an intestinal ILC2-epithelial response circuit. *Nature*. 2016;529:221–225.

58. Nadjsombati MS, McGinty JW, Lyons-Cohen MR, Jaffe JB, DiPeso L, Schneider C, Miller CN, Pollack JL, Nagana Gowda GA, Fontana MF, Erle DJ, Anderson MS, Locksley RM, Raftery D, and von Moltke J. Detection of succinate by intestinal tuft cells triggers a Type 2 innate immune circuit. *Immunity*. 2018;49:33–41.

59. Valderrama JA, Riestra AM, Gao NJ, LaRock CN, Gupta N, Ali SR, Hoffman HM, Ghosh P, Nizet V. Group A streptococcal M protein activates the NLRP3 inflammasome. *Nat. Microbiol*. 2017;2: 1425-34.

60. Gratz N, Siller M, Schaljo B, Pirzada ZA, Gattermeier I, Vojtek I, Kirschning CJ, Wagner H, Akira S, Charpentier E, and Kovarik P. Group A Streptococcus activates type I interferon production and MyD88-dependent signaling without involvement of TLR2, TLR4, and TLR9. *J Biol Chem*. 2008;283: 19879–19887.

61. Harder J, Franchi L, Munoz-Planillo R, Park JH, Reimer T, and Nunez G. Activation of the Nlrp3 inflammasome by Streptococcus pyogenes requires streptolysin O and NF-kappa B activation but proceeds independently of TLR signaling and P2X7 receptor. *J Immunol*. 2009;183: 5823–5829.

62. Loof TG, Goldmann O, and Medina E. Immune recognition of Streptococcus pyogenes by dendritic cells. *Infect Immun*. 2008;76: 2785–2792.

63. Hampton AL, Hish GA, Aslam MN, Rothman ED, Bergin IL, Patterson KA, Naik M, Paruchuri T, Varani J, and Rush HG. Progression of ulcerative dermatitis lesions in C57BL/6Crl mice and the development of a scoring system for dermatitis lesions. *J Am Assoc Lab Anim Sci*. 2012;51(5):586-93.

64. Williams LK, Csaki LS, Cantor RM, Reue K, Lawson GW. Ulcerative dermatitis in C57BL/6 mice exhibits an oxidative stress response consistent with normal wound healing. Comp Med. 2012 Jun;62(3):166-71.

65. Kastenmayer RJ, Fain MA, Perdue KA. 2006. A retrospective study of idiopathic ulcerative dermatitis in mice with a C57BL/6 background. J Am Assoc Lab Anim Sci 45:8–12

66. Mukai K, Matsuoka K, Taya C, Suzuki H, Nishioka K, Hirokawa K, Etori M, Yamashita M, Kubota T, Minegishi Y, Yonegawa H, and Karasuyama H. Basophils play a critical role in the development of IgE-mediated chronic allergic inflammation independently of T cells and mast cells. *Immunity*. 2005;23(2):191-202.

67. Obata K, Mukai K, Tsujimura Y, Ishiwata K, Kawano Y, Minegishi Y, Watanabe N, and Karasuyama H. Basophils are essential initiators of a novel type of chronic allergic inflammation. *Blood*. 2007;110(3): 913-920.

68. Matsuoka K, Shitara H, Taya C, Kohno K, Kikkawa Y, and Yonekawa H. Novel basophil- or eosinophil-depleted mouse models for functional analyses of allergic inflammation. *PLoS One*. 2013;8(4):e60958.

69. Cardona V, Guilarte M, Luengo O, Labrador-Horrillo M, Sala-Cunill A, and Garriga T. Allergic diseases in the elderly. *Clin Transl Allergy*. 2011;1:11.

70. Langfelder K, Streibel M, Jahn B, Haase G, Brakhage AA. Biosynthesis of fungal melanins and their importance for human pathogenic fungi. *Fungal Genet Biol.* 2003;38(2):143-58.

71. Mimura T, Itoh S, Tsujikawa K, Nakajima H, Satake M, Kohama Y, and Okabe M. Studies on biological activities of melanin from marine animals. V. Anti-inflammatory activity of low-molecular-weight melanoprotein from squid (Fr. SM II) . *Chem Pharm Bull*. 1987;35:1144–50.

72. Kunwar A, Adhikary B, Jayakumar S, Barik A, Chattopadhya S, Raghukumar S, and Priyadarsini KI. Melanin, a promising radioprotector: mechanisms of actions in a mice model. *Toxicol Appl Pharmacol*. 2012;264(2):202-11.

73. Ma Q, and He X. Molecular basis of electrophilic and oxidative defense: promises and perils of Nrf2. *Pharmacol Rev.* 2012;64(4):1055–81.

74. Love MI, Huber W, and Anders S. Moderated estimation of fold change and dispersion for RNA-seq data with DESeq2. *Genome Biol*. 2014;15:550.